CHIMIKA CHRONIKA

NEW SERIES

AN INTERNATIONAL EDITION
OF THE ASSOCIATION OF GREEK CHEMISTS

2/95

CMCRCZ 24(2), 77-172(1995)

ISSN 0366-693X

Volume 24, No 2 p.p. 77-172 April-June 1995

CHIMIKA CHRONIKA

NEW SERIES

AN INTERNATIONAL EDITION

Published by the Association of Greek Chemists (A.G.C.)
27 Kaningos str. Athens 106 82 Greece

Correspondence, submission of papers, subscriptions, renewals and changes of address should be sent to Chimika Chronika-New Series, 27 Kaningos street, Athens 106 82, Greece. The Guide to Authors is published in the first issue of each volume, or sent by request. Subscriptions: 25 USD per year.

Phototypesetted and Printed in Greece by EPTALOFOS S.A.
12, Arditou Str. 116 36 ATHENS Tel. 9217.513

Υπεύθυνος σύμφωνα με το νόμο: Ν. Κατσαρός, Κάνιγγος 27, Αθήνα 106 82.

Responsible under law: N. Katsaros, 27 Kaningos St., Athens 106 82, Greece.

Chimika Chronika, New Series, 24, 77-94 (1995)

STUDIES ON THE ROLES OF THE HYDROPHILIC AND HYDROPPHOBIC MOIETIES OF OXYTOCIN AND VASOPRESSIN. A PATHWAY LEADING TO ANTIOXYTOCIC ACTIVITY*.

Dimitrios Theodoropoulos[1] and Paul Cordopatis[2]

Departments of Chemistry[1] and Pharmacy[2], University of Patras, Greece.

Received: January 18, 1995

Dedicated to the memory of Professors A. Cosmatos and A. Galinos.

Running Title: Structure-Activity Studies on Neurohypophyseal Peptide Hormones.

* Abbreviations are according to the IUPAC-IUB Commission for biochemical nomenclature Eur. J. Biochem. *138,* 9 (1984); additional abbreviations are explained in the text. All optically active amino acids are of the L-configuration. pA_2 is the negative log of the antagonist concentration which reduces the response of a double dose of agonist to that of a single dose.

STUDIES ON THE ROLES OF THE HYDROPHILIC AND HYDROPHOBIC MOIETIES OF OXYTOCIN AND VASOPRESSIN. A PATHWAY LEADING TO ANTIOXYTOCIC ACTIVITY.

Summary

A systematic effort to relate the proposed three-dimentional structure of the neurohypophyseal hormones oxytocin and vasopressin to their biological activity, has led, from our part, to synthetic analogs with specifically modified activity profiles. These analogs were prepared either by solid phase synthesis or individual couplings in solution and resulted from modifications in the 20-membered ring structure or/and the flexible terminal portion of the hormones. Topological differences in the hydrophilic-hydrophobic balance of the hormone molecules account for differences in specific activity.

In view of the importance of oxytocin inhibitors for utilization clinically as tocolytics in cases of preterm delivery or threatened abortion, the general requirements for the design of antioxytocic peptides are also discussed. Emphasis is given in the conversion of weak agonists to antagonists by examination of positions 3 and 5 of the cyclic portion of the molecule, which were also found to be critical to the antagonistic activity.

Key words: Oxytocin, Vasopressin, Analogs, Structure-Activity Studies.

In a series of excellent papers, Roderich Walter, through his creative imagination, developed a hypothesis about the active model for the neurohypophyseal hormone Oxytocin (OT) while is bound to its uterotonic receptor (1, 2, 3). This model (Fig. 1) was based within the limits of conformational studies of the oxytocin molecule with NMR studies in dimethylsulfoxide. One surface of the molecular structure of OT is the hydrophobic edge, which consists of the side chains of the residues in the corner positions of the β-turns 3, 4, 7 and 8 and contain the "binding elements". The side chains of these residues are free for intermolecular interactions and it was suggested to be determinants of the differential specificity of the hormone-receptor interactions. The other side of the structure is the hydrophilic surface and consists of the hydroxyl group of Tyr^2 and the carboxamide groups of Gln^4, Asn^5 and Gly^9, which are primarily involved in the intramolecular stabilization of the peptide backbone. The Tyr^2 residue is folded over that side of the 20-membered covalent ring moiety of the hormone, already bearing the other aforementioned hydrophilic groups. The Tyr^2 side chain retains freedom of rotation and it was suggested that this phenolic hydroxyl group, in conjuction with the free carboxamide groups, form an "active center" of the hormone (4).

In $Arginine^8$-vasopressin (AVP) or $Lysine^8$-vasopressin (LVP) the side chain of Tyr^2 is away of the ring and is not part of the hydrophilic cluster, which consists of the carboxamides of Gln^4, Asn^5, Gly^9 and the basic moiety of residue 8. This is a fundamental difference between the oxytocin and vasopressin models (Fig. 2). The latter model includes also the stacking interaction of the aromatic rings of Tyr^2 and Phe^3. In general, positions 3, 4, 7 and 8 which are not primarily involved in the intramolecular stabilization of the

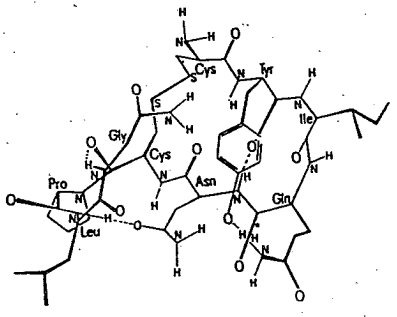

Figure 1. Proposed biologically active conformation of oxytocin while bound to its uterotonic receptor.

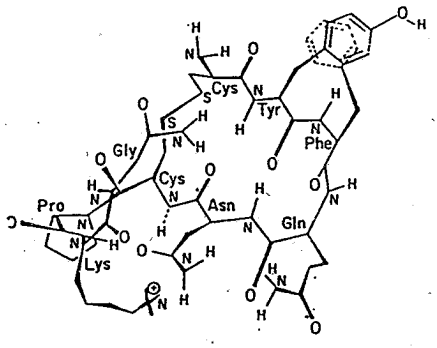

Figure 2. Proposed biologically active conformation of Lys^8 - vasopressin while bound to its antidiuretic receptor.

peptide backbone and, therefore, are available for intermolecular interactions, would lead to analogs with selectively modified activity profiles.

Structure-activity studies had shown, prior to 1978, that substitution of Asn^5 by other amino acids gave analogs with dramatically reduced uterotonic activity. However, the contribution of the Asn^5 residue to affinity and intrinsic activity was not clearly understood. As topological differences through changes in the hydrophobic-hydrophilic balance indicated to be of crucial importance, in 1977-1978, we became, at first, interested in oxytocin and vasopressin analogs bearing carboxamide side chains modified with hydrophobic groups. Thus, N^4, N^4-dialkylasparagine and N^5, N^5-dialkylglutamine were synthesized and used succesfully for the preparation of related neurohypophyseal analogs (5).

During this exploration, initially with R. Walter, I. Schwartz and C. Smith, the analogs of Table I were synthesized and the results of their studies are summarized as following:

Analog1. The exchange of the amino acid residues in positions 5 and 6 of oxytocin provides a 17-membered ring structure for the resulting analog, which devoids agonistic or antagonistic activity in the whole spectrum of the biological activities of the OT molecule. Is, therefore, becaming apparent that the 5-position of Asn is crusial for producing conformational restrictions recognizable to receptor sites (6).

Analog 2. Synthetic [5-(N^4, N^4-dimethylasparagine)] OT possesses 4.60+0.030 U/mg uterotonic activity, but most important, it displays an identical intrinsic activity *in vitro* as oxytocin. This finding is a clear experimental evidence that in OT the 5 position of the Asn residue contains an "active element" responsible for the intrinsic activity. Therefore, the significance of the carbonyl group in the

Table I. Synthetic Analogs of Oxytocin and Vasopressin

1. H-Cys-Tyr-Ile-Gln-Cys-Asn-Pro-Leu-Gly-NH_2
   [5-cysteine, 6-asparagine] oxytocin
2. H-Cys-Tyr-Ile-Gln-Asp[$N(CH_3)_2$]-Cys-Pro-Leu-Gly-NH_2
   [5-(N^4, N^4-dimethylasparagine)] oxytocin
3. H-Cys-Tyr-Phe-Gln-Asp[$N(CH_3)_2$]-Cys-Pro-Lys-Gly-NH_2
   [5-(N^4, N^4-dimethylasparagine), 8-lysine] vasopressin
4. H-Cys-Tyr-Ile-Glu[$N(CH_3)_2$]-Asn-Cys-Pro-Leu-Gly-NH_2
   [4-(N^5, N^5-dimethylglutamine) oxytocin
5. H-Cys-Tyr-Ile-Glu[$N(n\text{-}C_3H_7)_2$]-Asn-Cys-Pro-Leu-Gly-NH_2
   [4-(N^5, N^5-di-n-propylglutamine)]oxytocin
6. H-Cys-Tyr-Phe-Glu[$N(CH_3)_2$]-Asn-Cys-Pro-Lys-Gly-NH_2
   [4-(N^5, N^5-dimethylglutamine), 8-lysine] vasopressin
7. H- Cys-Tyr-Ile-Glu[$N(CH_3)_2$]-Asp[$N(CH_3)_2$]-Cys-Pro-Leu-Gly-NH_2
   [4-(N^5,N^5-dimethylglutamine), 5(N^4, N^4-dimethylasparagine)]oxytocin
8. H-Cys-Tyr-Ile-Glu($NHNH_2$)-Asn-Cys-Pro-Leu-Gly-NH_2
   [4-(glutamic γ-hydrazide)] oxytocin
9. H-Cys-Tyr-Phe-Glu($NHNH_2$)-Asn-Cys-Pro-Lys-Gly-NH_2
   [4-(glutamic γ-hydrazide), 8-lysine]vasopressin
10. H-Cys-Tyr-Ile-Gln-Asn-Cys-Pro-Leu-Gly-$N(CH_3)_2$
    Oxytocinoic acid dimethylamide
11. H-Cys-Tyr-Phe-Gln-Asn-Cys-Pro-Leu-β-Ala-NH_2
    [9-β-alanine] oxypressin
12. H-Cys-Tyr-Thr (Me)-Gln-Asn-Cys-Pro-Leu-Gly-NH_2
    [3-O-methylthreonine] oxytocin
13. H-Cys-Tyr-Ser (Et)-Gln-Asn-Cys-Pro-Leu-Gly-NH_2
    [3-O-ethylserine] oxytocin
14. H-Cys-Tyr-Hse (Me)-Gln-Asn-Cys-Pro-Leu-Gly-NH_2
    [3-O-methyhomoserine] oxytocin

γ-position of the side chain is apparent. Thus the Asn^5 residue has the dual function to stabilize the three-dimentional conformation and to contribute an active element (7).

Analog 3. In the proposed biologically active conformation of vasopressin at the antidiuretic receptor, the 5-position asparaginyl residue seems to play an important role. The side-chain carboxamide group acting cooperatively with the basic moiety of the 8-position residue have been suggested to be the "active elements" of the hormone. This is demonstrated by the lack of antidiuretic activity of [5-alanine, 8-lysine]-vasopressin. In this connection, the [5-(N^4, N^4-dimethylasparagine), 8-lysine]-vasopressin is the first 5-position analog to retain significant potency in this assay, indicating that the carbonyl group and no the hydrogen atoms of the - $CONH_2$ group, is essential for activity (8).

Analogs 4,5,6. Conformational data imply that when OT is bound to the uterotonic receptor, the orientation of the side chain at position 4 is toward the "active elements" and reaches into the active cavity. Therefore, the effects on the biological activities of substituting the carboxamide hydrogen atoms of Gln^4 by bulky groups was investigated. Indeed, biological evaluation of certain synthetic N^5-N^5-dialkylglutamine analogs (No 4, 5, 6) indicate in the rat uterotonic assay greater diminished intrinsic activity with increazed steric size at the 4-position side chain. Concerning the reduced antidiuretic potency of the [N^4, N^4-dimethylglutamine]LVP analog it is not clear yet whether is due to loss of affinity or intrinsic activity (9).

Analog 7. The biological findings of [5-(N^4, N^4- dimethylasparagine]OT prompted us to synthesize and evaluate the introduction of a second ω-dimethylamide in position 4. Thus, [4-(N^5, N^5-dimethylglutamine), 5-(N^4, N^4-dimethylasparagine)]OT was synthesized and its structure was fully

characterized by liquid secondary mass ion spectroscopy. This was an encouraging example of identifying complex peptide structure by this technique. The introduction of the second ω-dimethylamide caused severe consequences on the biological activities of this OT-analog, which was found to be almost inactive in the uterotonic, antidiuretic, pressor and milk ejection assays (10).

Analogs 8, 9. To further explore the effect (s) of a minimal change of the carboxamide group of Gln^4 of OT and LVP without altering the hydrophilic character of this group, one hydrogen atom of the $CONH_2$was replaced with NH_2-group. The resulting analogs [4-Clu($NHNH_2$)] OT and [4-Glu($NHNH_2$)] LVP were synthesized. The biological data of these analogs indicate that the hydrazide substitution in the oxytocin molecule decreases moderately the milk ejection, but decreases the uterine contraction more severely. The antidiuretic activity of the [4- Glu($NHNH_2$)] LVP analog is moderately decreased, in contrast to different shortenings of the side chain of Gln^4, which are not tolerated. The hydrazide substitution is also tolerated by the pressor receptor. In comparison with relevant analogs, another difference between the antidiuretic and pressor receptors is that some electronegativity seems to be required in position 4 for pressor activity (11).

Analog 10. Oxytocinoic acid dimethylamide was synthesized and its pharmacological properties were compared to those of oxytocin. The analog exhibits 3% of the potency of oxytocin in the *in vitro* uterotonic assay. This finding suggests that the replacement of the hydrogen atoms of the C-terminal carboxamide of OT by the bulky and hydrophobic methyl groups affects the proper orientation of the "active elements" in the hydrophilic cluster. In the *in vitro* uterotonic assay, oxytocinoic acid dimethylamide showed a reduced

affinity for the oxytocin receptor, a nonparallel dose-responce relationship, and most important a reduced intrinsic activity as compared to oxytocin. In the avian vasodepressor, rat pressor and rat antidiuretic assays the analog was almost inactive (12).

Analog 11. In this analog the glycine residue in position 9 has been replaced by β-alanine. The insertion of a CH_2 group in position 9 seems to deorientate the C-terminal carboxamide group from its optimal position in the active center. Thus, the analog exhibits reduced uterotonic, antidiuretic and pressor activity, compared to oxytocin, oxypressin and [8-Alanine] oxypressin. It should be noted that replacement of glycine by β-alanine results in greater conformation freedom of the C-terminal tripeptide Pro-Leu-β-Ala-NH_2 leading, thus, to quite different biological responces (13, 14, 15).

Analogs 12,13,14. The side chain of Ile in position 3 of oxytocin occupies the first corner position of the type II β-turn and hence an equatorial position. A number of analogs, in which the aliphatic isoleucine residue has been substituted by other aliphatic side chains, indicate, in dose-responce experiments, differences in receptor affinity alone. These results add evidence for position 3 as a binding site. Since the aliphatic side chain of Ile^3 devoids of any polarity, we decided to insert a polarized, and therefore hydrophilic oxygen atom into the hydrophobic chain. Using O-ethylserine, O-methylthreonine and O-methylhomoserine (16, 17) instead of isoleucine, the three analogs [3-O-ethylserine]OT, [3-O-methylthreonine]OT and [3-O-methylhomoserine]OT were synthesized and tested for potencies and specificities. In these analogs the electronegative atom is placed in different distances from the peptide backbone. The position of the electonegative atom is rather important to antidiuretic activity. Although all three analogs have low

pressor activity, moving the oxygen further from the peptide backbone this activity is decreased, but, in contrast, has no effect on oxytocin-like activities. Another finding of this study is the moderately higher milk ejection of [3-Hse]OT than that of oxytocin. This, support the assumption that the galactogonic receptor does not have such strict structural requirements as the other receptors for oxytocin (18).

Antagonists: Oxytocin analogs with inhibitory properties not only are valuable tools for the evaluation of the action mechanism of this hormone, but they can also be utilized in clinical practice as tocolytics in cases of preterm delivery or threatened abortion. An effective inhibitor has dual role, to block direct action of oxytocin on myometrial contractions as well as to prevent prostaglandin release by oxytocin stimulated uterus. Up to date the structural features leading to oxytocin inhibitors can briefly summarized as following:

1. Replacement of the hemicystine residue in position 1 by a penicillamine (Pen) derivative for increazed rigitation of the molecule, since the disulfide ring is more flexible.

2. Change of configuration of amino acid in position 2 (D-amino acid), deletion of the OH group of Tyr^2 or its replacement by a more lipophilic residue.

3. Substitution of glutamine in position 4, by threonin, proline in position 7 by dehydroproline and leucine in position 8 by basic amino acid.

4. Positions 2 and 5 should be fixed, such that one or both side chains cannot orient over the 20-membered disulfide ring.

5. Carba substitution for disulfide bridge influences the antagonistic properties, a fact which has been previously observed with agonists (19).

It should be emphasized that only one single substitution, from those referred above, does not lead to *in vivo* strong inhibitors. In general, agonists

and antagonists appear to use different structural and conformational features for interaction with the uterine receptor (5).

From conformational studies positions 2, 4 and 8 affect factors like affinity to the receptor and metabolic stability. Conformational restriction at position 7 (dehydroproline) provides antagonists with prolonged activity. Nevertheless, the enzymic cleavage of the linear C-terminal tripeptide by a post-proline enzyme is of major importance in living organisms. The Pro^7 residue occupies the one corner of the β-fold which, in contrast to positions 3, 4 and 8, has not been found to be substituted by other amino acid in the course of evolution of the neyrohypophyseal hormones. Also, the Pro^7 residue is located in the enzymatically vulnerable part of the hormones and substitution of this residue may yield analogs, which render the acyclic peptide portion more resistant to enzymatic attack (20).

A great number of oxytocin antagonists have been designed, synthesized and tested in several assay systems not only *in vitro* but *in vivo* systems as well. Some of them have been used as pharmacological tools to asses the role of oxytocin in labor and as an inhibitor of uterine contractions during preterm labor. It should be mentioned that the Swedish Ferring Research Institute was the first to introduce in the market the inhibitor **Atosiban** and its further modified analogs (21).

Mpa-D-Tyr(Et)-Ile-Thr-Asn-Cys-Pro-Orn-Gly-NH_2

Mpa=3-mercaptopropionic acid

Another inhibitor named **Carthetocin** was introduced into veterinary practice as a drug with selective uterotonic and milk-ejecting action (22).

[Deamino-1-carba, 2-O-methyltyrosine]oxytocin

Carthetocin

Also potent inhibitor *in vivo* systems, named **Antag** has been obtained when Tyr^2 was replaced with $D\text{-}Tyr^2$ (23).

[1-PMP, 2-D-Trp, 8-Arg]-oxytocin pA_2=7.73

PMP=β, β-Cyclopentamethylene-β-mercaptopropionic acid.

Conformational constrains which increase the rigidity of structure of both the peptide backbone and several amino-acid side chains group seems to afford strong inhibitors as indicate by the bicyclization of the weak monocyclic analog **a** to **b** (24).

a. [1-β-Mpa, 4-Glu, 6-Cys, 8-Lys]-oxytocin

b. [1-β-Mpa, 4-Glu, 6-Cys, 8-Lys]-oxytocin

pA_2=8.2+0.2

Among the highly potent antagonists it should be mentioned the recently reported by Hruby (25) as result of his previous systematic studies.

[1-Pen, 2-D-Phe, 4-Thr, 5-Thr, 6-Cys, 8-Orn]-oxytocin

It is apparent from the already mentioned typical examples of strong inhibitors, that all these have been obtained by complex and drastic modifications of the oxytocin molecule, which affect backbone conformation and impose rigidity of structure. We hypothesized that minimal changes in the cyclic portion of the proposed biologically active model of oxytocin may provide keen information concerning the structure-activity relationships of antagonists. This in turn may facilitate the design of structures without the need of gem-substitution at the β-carbon atom in position 1 and most important with greater potency, as well as longer duration of action.

It has been previously referred to the "cooperative model" for oxytocin (4) and our experimental evidence that the hydrogens of the N^4-amine portion of the asparaginyl side chain are not essential for oxytocin-like activities (7). On the contrary the importance of the carbonyl group of Asn^5 in γ-position as an"active element" which in cooperation with the hydroxyl group of Tyr^2 initiates oxytocin activity, became apparent from our synthetic analogs. Thus [5-(N^4, N^4-dimethylasparagine)]OT possesses a uterotonic potency of 4.60+0.5, but most important indicates the same intrinsic activity as oxytocin. Furthermore when the alkyl substituents are made larger and thus the steric hindrance around the carbonyl group of Asn^5 was increased, nearly inactive analogs were obtained, e.g. [5-(N^4, N^4- diisopropylasparagine)]OT (26).

It is well known that any modification in position 5 of oxytocin results in analogs with almost no activity. However analogs with hydrophilic instead of hydrophobic side chains in positions 5, indicate less negligible potency (Table II).

Table II. Synthetic Analogs of Oxytocin Modified in Position 5.

1.	oxytocin (OT)	546 (in vitro rat uterotonic potency)
2.	[5-alanine]OT	0.05
3.	[5-valine]OT	0.20-0.030
4.	[5-serine]OT	0.70
5.	[5-glutanine]OT	1.00
6.	[5-(N^4, N^4- dimethylasparagine)]OT	4.60+0.003

In our experience [5-threonine]OT indicates also uterotonic *in vitro* activity of 0.45 + 0.15 IU/mg. Therefore, we were intrigued by the possibility that increasing of the electronegativity of the oxygen atom of the weak agonists [5-serine]OT (27) and [5-threonine]OT may strengthen its hydrogen acceptan character and consequently enhance the oxytocic action. Thus, O-methylated serine and threonine were used for the preparation of [(OMe)Ser^5]OT and [(OMe)Thr^5]OT. Surprisingly, the methylated analogs, in contrast to their non-methylated weak agonists, were transformed to pure weak antagonists. For example, [(OMe)Ser^5]OT and [(OMe)Thr^5]OT indicated pA_2 values of 5.7 and 5.8 in the *in vitro* rat uterotonic assay. Both weak antagonists were found to be inactive in the pressor and galactogonic assays (28). In our experience, this is the first 5 position minimal modification in OT which results in antagonistic action. A plausible explanation from the point of view of the directionality of the hydrogen bond may be given. In contrast to weaker van der Waals forces involved in hydrophobic bonding, hydrogen bonds are directional and therefore bind two atoms in a specific orientation toward each other. Nevertheless due to + I effect of the methyl group the electron density of the oxygen atom of Thr^5 is increased, but in the mean time the methyl group may hinder the proton transfer from the hydroxyl group of Tyr^2 to the oxygen atom of the hydroxyl groups of Ser^5 and Thr^5. It appears, therefore, that the active elements involved in receptor stimulation do not obtain the minimum of a proper orientation for productive interaction with the receptor and this may be related with the antagonistic action.

Another modification involving binding but not receptor stimulation was undertaken. Since the residue in position 3 (Ile^3) occupies the first corner

position of the β-turn and is primarily important for receptor binding, we substituted Ile^3 with Aib^3, which is known to introduce considerable constrains on the backbone of the 20-membered ring of OT. Interestingly, the resulting analog [Aib^3]OT (Aib; α-aminoisobutyric acid or α-methylalanine) was found to be a weak antagonist with pA_2 value of 5.9 and not detectable pressor and galactogonic activity. Whether the Aib^3 modification affects only binding or even hinters the receptor stimulation through deorientation of the active elements is not clear yet. The accumulation of these minor modifitions in one molecule and the extention of investigations to include additional corner positions-with particular emphasis on antioxytocic activity-should prove to be instructive.

Περίληψη

ΜΕΛΕΤΕΣ ΤΟΥ ΡΟΛΟΥ ΤΩΝ ΥΔΡΟΦΙΛΩΝ ΚΑΙ ΥΔΡΟΦΟΒΩΝ ΠΕΡΙΟΧΩΝ ΤΗΣ ΩΚΥΤΟΚΙΝΗΣ ΚΑΙ ΒΑΣΟΠΡΕΣΣΙΝΗΣ. ΜΙΑ ΣΤΑΔΙΑΚΗ ΠΟΡΕΙΑ Η ΟΠΟΙΑ ΚΑΤΑΛΗΓΕΙ ΣΕ ΑΝΤΙΩΚΥΤΟΚΕΙΟ ΔΡΑΣΗ.

Μια συστηματική εκ μέρους μας προσπάθεια να συσχετίσουμε την προταθείσα τριδιάστατη δομή των ορμονών της νευροϋποφύσεως ωκυτοκίνη και βασοπρεσσίνη, οδήγησε στη σύνθεση ενός αριθμού "αναλόγων" με διαφοροποιημένη κατανομή βιολογικών ιδιοτήτων.

Τα εν λόγω "ανάλογα" συνετέθησαν με εφαρμογή της μεθοδολογίας πεπτιδικής συνθέσεως επί στερεάς φάσεως ή με καταλλήλους μεθόδους συζεύξεως σε υγρή φάση. Η τοπικώς επιφερομένη διατάραξη της υδροφίλου-υδροφόβου ισορροπίας συνεπάγεται διαφοροποιήσεις στο φάσμα των ειδικών βιολογικών δράσεων.

Δεδομένης της σημασίας των ανταγωνιστών της ωκυτοκίνης για κλινική χρήση σε περιπτώσεις προώρου τοκετού ή γενικά κινδύνου

αποβολής του εμβρύου, αναφέρονται βασικές αρχές σχεδιασμού πεπτιδίων με αντι-ωκυτόκειο δράση. Εμφαση δίνεται στη μετατροπή ασθενών "αγωνιστών" σε "ανταγωνιστές" οι οποίοι, όπως διαπιστώσαμε, λαμβάνονται με απλές τροποποιήσεις στις θέσεις 3 και 5 του κυκλικού τμήματος του μορίου της ωκυτοκίνης. Τα δεδομένα αυτά, συνδυάζονται με άλλες τροποποιήσεις σε β-στροφές του μορίου, οι οποίες ευρίσκονται σε εξέλιξη.

REFERENCES

1. Walter, R.: Margoulies, M. and Greenword, F. (Eds.).: *Structure Activity Relationships of Protein and Polypeptide Hormones,* p. 181, (Eds.) Experpta Medica Foundation, Amsterdam, 1971.
2. Urry, D. and Walter, R. : *Proc.Natl.Acad.Sci. U.S.A.,* **68,** 956 (1971).
3. Walter, R., Schwartz, I., Darnell, J. and Urry, D. : *Proc. Natl. Acad. Sci. U.S.A.,* **68**, 1355 (1971).
4. Walter, R: *Fed. Proc.* **36**, 1872 (1977).
5. Caplaneris, Th., Cordopatis, P., Matsoukas J. and Theodoropoulos, D. : *Tetrahedron,* **34**, 969 (1978).
6. Theodoropoulos, D., Liakopoulou, M. and Smith, C. : Loffet, A. (Ed.).: *Peptides 1976,* p. 505, Editions de l' Universite de Bruxelles, 1976.
7. Walter, R., Stahl, G., Caplaneris, Th., Cordopatis P., and Theodoropoulos D.: *J. Med. Chem.*, **22**, 890 (1979).
8. Smith, C., Walter, R., Stavropoulos G. and Theodoropoulos D. : *J. Med. Chem.,* **23**, 217 (1980).
9. Stahl, G., Smith, C., Walter, R., Tsegenidis, T., Stavropoulos, G., Cordopatis, P. and Theodoropoulos, D. : *J. Med Chem.,* **23**, 213 (1980).

10. Theodoropoulos, D., Cordopatis, P., Dalietos, D., Furst A. and Lee T.: *Eur. J. Med. Chem.*, **22**, 453 (1987).

11. Gazis, D., Glass, J., Schwartz, I., Stavropoulos G., and Theodoropoulos, D. : *Int. J. Peptide Protein Res.*, **34**, 353 (1989).

12. Ting, Y., Smith, C., Stahl, G., Walter, R., Cordopatis, P. and Theodoropoulos, D. : *J. Med. Chem.*, **23**, 693 (1980).

13. Anagnostaras, P., Cordopatis, P. and Theodoropoulos, D. : *Eur. J. Med. Chem.*, **16**, 171 (1981).

14. Anagnostaras, P., Cordopatis, P. Matsoukas, J., Stavropoulos, G. and Theodoropoulos, D. : *Tetrahedron*, **34**, 973 (1978).

15. Matsoukas, J., Cordopatis, P. and Theodoropoulos, D. : *J. Org. Chem*, **42**, 2105 (1977).

16. Barlos, K. and Theodoropoulos D. : *Z. Naturforsch.*, **37**, 886 (1982).

17. Barlos, K., Papaioannou, D., Cordopatis P. and Theodoropoulos, D. : *Tetrahedron*, **39**, 475 (1983).

18. Gazis, D., Schwartz, I., Cordopatis P. and Theodoropoulos, D. : *Int. J. Peptide Protein Res.*, **27**, 679 (1986).

19. Lebl, M., Fric, I., Sugg, E., Cody, W. and Hruby, V. : Theodoropoulos, D. (Ed.): *Peptides 1986*, p.341 Walter de Gruyter, Berlin, 1987.

20. Walter, R., Yamanaka, T. and Sakakibara, S. : *Proc. Natl. Acad. Sci. U.S.A.*, **71**, 1901 (1974).

21. Aurell, C., Johansson, E., Persson, R., Berden, L., Nilsson, A., Trojnar, J., Abbe, M., Fkholm, K., Hansson, C., Nylen, A., Rosenqvist, A., Johansson, B., Persson, C. and Melin P. : Schneider, C and Eberle, A. (Eds.).: *Peptides 1992*, p. 697, ESCOM, Leiden, 1993.

22. Fric, I., Kodicek, M., Prochazka, Z., Jost, K., and Blaha, K. : *Collect. Czeh. Chem. Comm.*, **39**, 1290 (1974).

23. Flouret, G., Brieher, W., Mahan, K. and Wilson, L. :Jung, G. and Bayer, E. (Eds.): *Peptides 1988*, p. 549, Walter de Gruyter, Berlin, 1989.

24. Hill, P., Slaninova, J. and Hruby, V. : Marshall, G.: *Peptides, Proc., 10th American Peptide Symposim*, p. 468, ESCOM-Leiden, 1988.

25. Hill, S., Chan Y. and Hruby V. : *Int. J. Peptides and Proteins Res.*, **38**, 32 (1991) and references cited therein.

26. Cordopatis, P. and Theodoropoulos, D. : unpublished results.

27. Guttman, S. and Boissonnas, R. : *Helv. Chim. Acta*, **46**, 1626 (1963).

28. Assimomytis, N., Manessi-Zoupa, E., Cordopatis P. and Theodoropoulos, D.: *Collect. Czech. Chem. Comm.*, **59**, 718 (1994).

Chimika Chronika, New Series, 24, 95-114 (1995)

SUPRAMOLECULAR CHEMISTRY

E. Hadjoudis

Institute of Physical Chemistry

N.C.S.R. "Demokritos", 153 10

Aghia Paraskevi-Attiki, Greece

Running Title: SUPRAMOLECULAR CHEMISTRY

Received: February 20, 1995

SUPRAMOLECULAR CHEMISTRY

Summary: This paper describes briefly the development of supramolecular chemistry, elaborating the strategies towards properties and functions openning new horizons to the imagination of researchers.

Key words: carcerands, cyclodextrins, rotaxanes, catenanes, supramolecular catalysis, supramolecular applications.

INTRODUCTION

The increased communication between the various chemical disciplines which developed separately resulted, after reunification, in the development of a highly intergrated science the Supramolecular Chemistry, a new multi-disciplinary area at the cross-roads between the life sciences and material science.

Jean-Marie Lehn, in his Nobel Lecture, gave the following definition of the term: "Supramolecular Chemistry is the chemistry of the intermolecular bond, covering the structures and functions of the entities formed by association of two or more chemical species". Thus supramolecular species are constructed by combining molecular species in a similar way to molecules being obtained by the combination of atoms. Therefore, Supramolecular Chemistry is the chemistry beyond the molecule and deals mostly with noncovalent chemical bonds, i. e. electrostatic interactions, hydrogen bonding, van der Waals forces, etc. within a defined molecular architecture. The partners of a supramolecular species have been named molecular receptor and substrate, the substrate being usually the smaller component whose binding is being sought.

Binding of a substrate σ to its receptor ρ yields the supermolecule $\rho\sigma$ and involves a molecular recognition process. If the receptor bears reactive sites, it may effect a chemical transformation on the bound substrate, thus behaving as a catalyst, and a lipophilic membrane-soluble receptor may act as a carrier effecting the translocation of the bound substrate. Thus molecular recognition, transformation and translocation represent the basic functions of supramolecular

species. Functional supermolecules, in association with organized polymolecular assemblies and phases, may lead to the development of supramolecular devices[1].

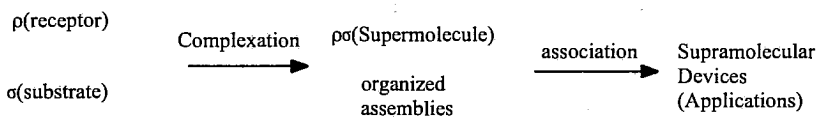

Supramolecular chemistry is rapidly expanding and enormous progress has been made during the last few years. However it is not possible to cover in an article the vast literature that has been developed and to justice the numerous results and provide an exhaustive account of this field. Therefore the purpose of this article is to demonstrate some typical supramolecular systems, which have been presented during the first decades of this new field, in such a way that its dynamism will be uncovered and be the subject of young innovative scientists.

In order to achieve this goal without the fear of fragmentation, we shall give examples under the following headlines:

Design and Synthesis of Supramolecular Systems, Self Assembly of Supramolecular Structures, Reactivity of Supramolecular Structures, Supramolecular Catalysis and Supramolecular Applications and Technology.

DESIGN AND SYNTHESIS OF SUPRAMOLECULAR SYSTEMS

The concept of intermolecular interactions is a very old one but new ideas about these interactions appear only in the end of the 19th century when Van der

Waals explained the nonideal behaviour of gases and Emil Fischer made his famous analogy between the way a substrate and enzyme interact to the way that a key fits into a lock[2] as it is illustrated in Fig. 1. The enzyme, which is large relative to the substrate, has clefts and depressions on its surface complementary to the shape of the substrate[3].

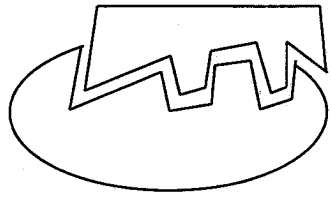

Fig. 1. Schematic representation of Fisher's Lock-Key Concept in an enzyme-substrate complex.

Synthetic chemists imitate the non-covalent interactions found in nature and pioneering work focused on cyclodextrin inclusion complexes and crown ether-metal ion interactions. Many subsequent studies used macrocycles (as cyclodextrins and crown ethers) by design under an intuitive sense that macrocycles experience fewer conformational restrictions upon complexation than their acyclic counterparts. This now embodied in Cram's principle of preorganization[4] which states that complex stability will be maximized when the constituent parts are structurally organized for complexation and low solvation.

Macrocycles have the additional benefit that their finite cavity dimensions make them inherently selective in binding due to size exclusion. The very large

rigid cavities required to bind large molecules are difficult to construct, although progress in this area has been reported[5].

The result of the rapid development of supramolecular chemistry is the synthesis[6] of host molecules of many highly-diverse structural forms as 1.

Cram has defined hosts and guests as organic molecules or ions whose binding sites converge and diverge, respectively, in forming a complex[7].

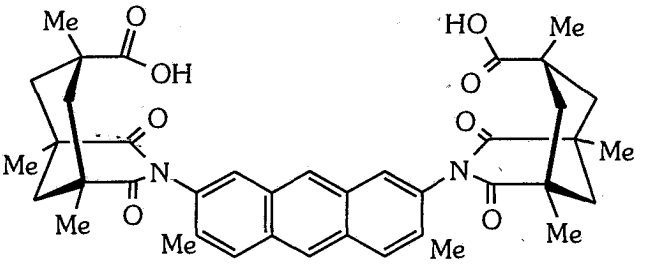

1

The design of molecules may be in such a way as to include a function as well as a form. An elegant demonstration of this approach is the supramolecular liquid crystal shown in Fig. 2. in which two complementary sub-units associate via hydrogen-bonding to form the rigid central element of the mesogenic supermolecule[8].

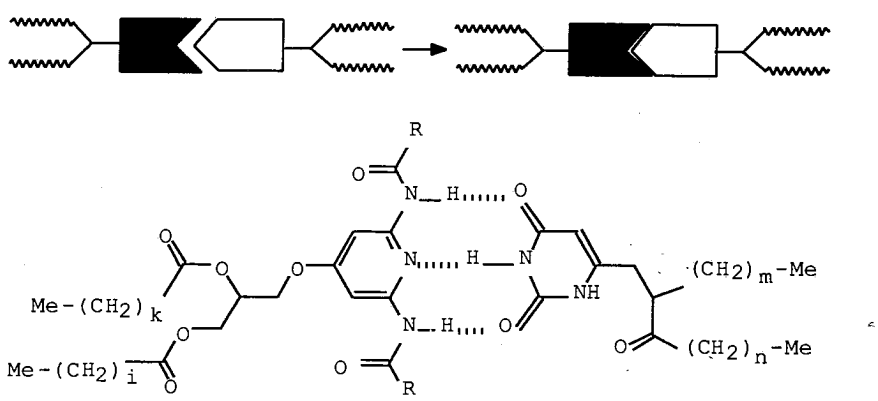

Fig. 2. Schematic representation of the formation of a mesogenic supramolecule in which hydrogen-bonding was used between two complementary sub-units to form a rigid central core[8].

Compounds with belt-type and cage-type structures are important in the development of supramolecular chemistry and many cage-type compounds have been prepared while the access to compounds of the calixresorcinarene class and the observation by Cram that the rigidity of the calixresorcinarenes can be increased resulted in the cavitand class of macropolycycles.

Further Cram considered the linking of two cavitands and the outcome was the synthesis of the first closed molecular container compounds, the carcerands[9]. Carcerands present extreme insolubility but

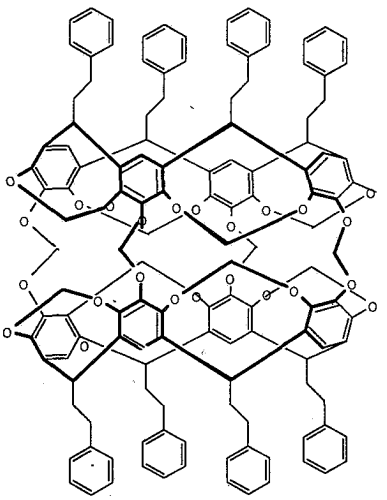

2

the addition of solubilizing lipophilic arms furnish compounds, such as structure 2, which allow N.M.R. spectroscopic analyses to be perfor-med on carcerands and to probe the behaviour of the encapsulated solvent molecules and also to act as slow-release drug-delivery systems and as targeted immunoprotein-associated chemotherapeutic agents.

We shall close this topic by mentioning the pioneering studies of Cramer on the molecular recognition characteristics of cyclodextrins which play an important role in the field of supramolecular chemistry and find applications in various fields of science and technology. The cyclomaltooligosaccharides (cyclodextrins, CDs) show a remarkable ability to form inclusion complexes with various natural and synthetic molecules. The inclusion process is influenced not only by the host-guest hydrophobic interactions but also by the shape, size and hydrogen-bonding ability of the guest. Depending on the size and molecular or ionic character of the guest, α-CD inclusion complexes crystallise in distinct

categories[10] and most β-CD inclusion complexes crystallise as dimers in four modes[11]. Fig. 3 shows the structure of α-CD and Fig. 4 the dimensions of the toroidal cavity of α-, β- and γ-CD in A.

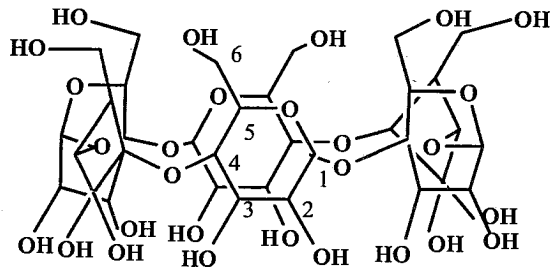

Fig. 3. Structure of α-cyclodextrin.

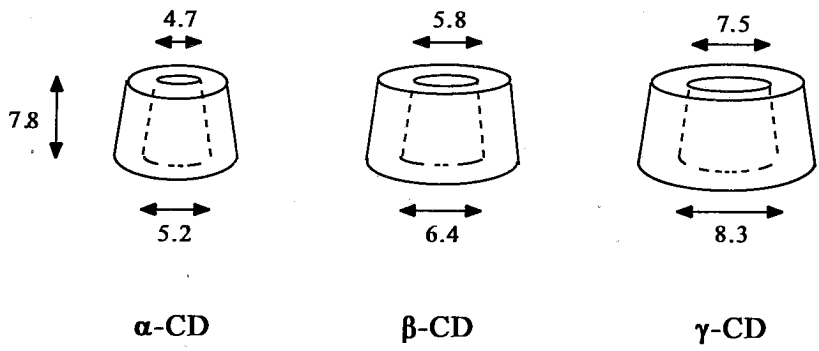

Fig. 4. Dimensions of the toroidal cavity of cyclodextrins in A.

The recent synthesis of a peranhydro α-cyclodextrin (5) provides a novel way of alteration of the structural properties of the cyclodextrin skeleton. The dehydration process forces each D-glucopyranose ring

out of its original $^4C_1$ in 3 to a $^1C_4$ chair conformation in 5, altering thus the nature of the cavity from a lipophilic environment to one flanked by glucosidic, glucopyranose, and free hydroxyl oxygen atoms which in turn alter the physical properties and binding characteristics of the cyclodextrin[6].

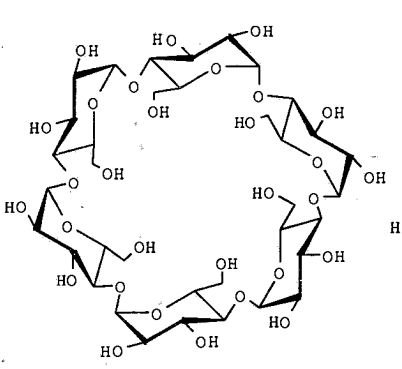

3

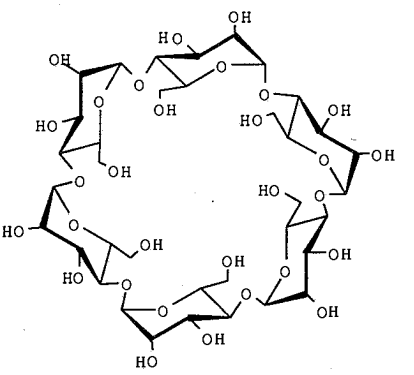

4

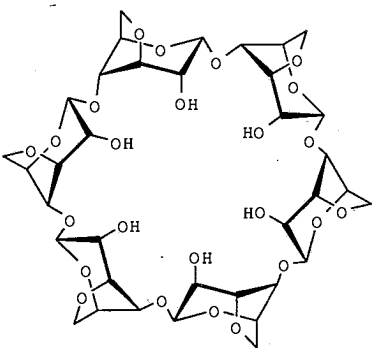

5

SELF ASSEMBLY OF SUPRAMOLECULAR STRUCTURES

Fraser Stoddart[12] stated that self-assembly and self-replication may be the secrets that synthetic chemists have to learn from nature to be able to constuct molecular electronic devices and he gave a personal account on the way he formulated a strategy for self-assembly processes that might aid and abet unnatural product synthesis. Fig. 5. shows how a catenane and rotaxane may be self assembled. Thus a [2]catenane can be made by (a) clipping

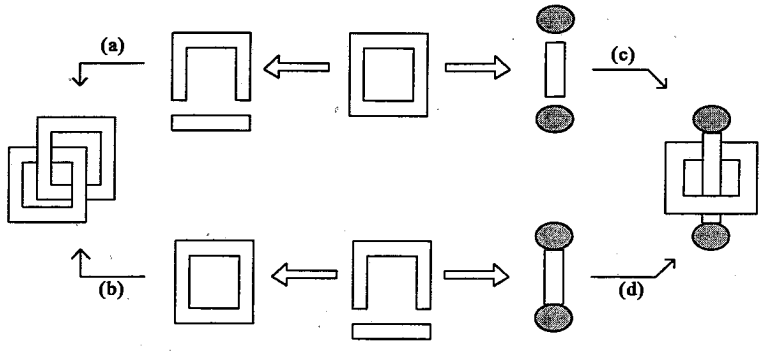

Fig. 5. Self-assembly of a [2]catenane and [2]rotaxane.

an unshaded ring around an already complete shaded ring, or (b) vice versa. A [2]rotaxane can be made by (c) threading a complete shaded ring with an unshaded rod and then covalently stoppering the ends of the rod with big black moons, or by (d) clipping a shaded ring around an unshaded rod that is already covalently stoppered at its ends with big black moons.

The clipping of a second ring round an already complete ring has been done and good stoppers have been discovered e.g. triisopropylsilyl group was a

good "stopper" for the ends of polyether chains containing hydroquinol units and an example of a molecular "shuttle" was prepared comprised of a [2]rotaxane where the molecular components are a bis(silyloxy-ethoxyethoxyethoxy-phenoxyethoxyethoxy) ether and cyclobis (paraquat-p-phenylene).

A number of template-directed syntheses of [2]rotaxanes and [2]catenanes illustrate that there are inherently simple ways of making apparently complex unnatural products from appropriate substrates without the need for reagent control or catalysis. Template synthesis of defined molecular cavities leads to "inclusion chemistry on a nanometer scale"[13].

The latest achievement in this field is the preparation of a linear chain of five interlocked rings, a [5]catenane, the structure of which resembles the symbol of the international Olympic Games and thus the name olympiadane has been adopted by professor Stoddart's group[14].

The prefix in square brackets before the name indicates the number of molecular components comprising these compounds that include "topological", as well as covalent bonds: e.g. [2]rotaxanes (Latin: rota=wheel, axis=axle) and [2]catenanes (Latin: catena=chain) are the simplest examples[15].

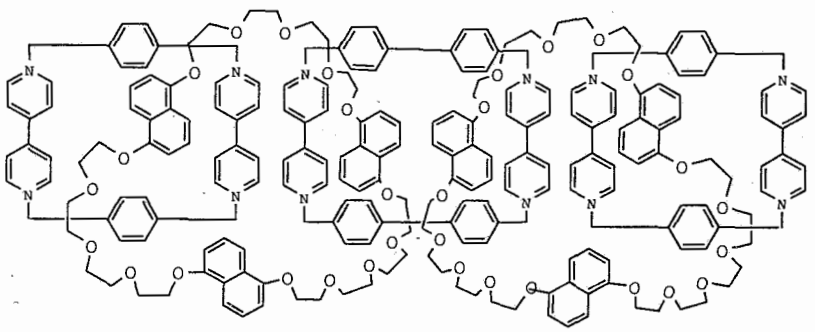

Olympiadane

REACTIVITY OF SUPRAMOLECULAR SYSTEMS

Supramolecular reactivity, the modification of chemical and/or physical properties of the bound substrate results from the formation of a receptor-substrate (or host-guest) complex and may be tuned by changing the structure of the receptor (host) molecule. The design of specific complexing components may generate specific chemical and physical reactivities leading to new and/or controlled properties[16]. Thus J. M. Lehn showed that europium cryptates of macrobicyclic ligands luminesce under direct excitation of the cation in conditions in which the free ion does not emit[17] (Fig. 6).

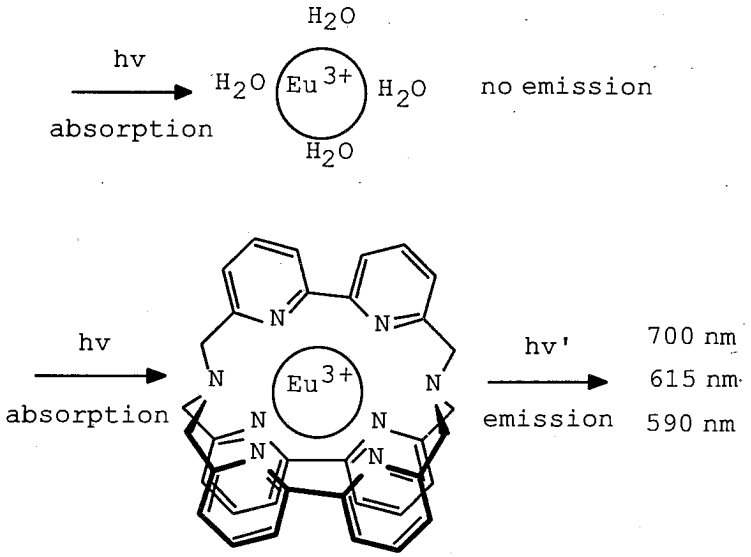

Fig. 6. Light conversion process performed by the cryptate [Eu(III):bipy.bipy.bipy] (bipy = 2,2'-bipyridine).

Numerous results have been reported on the effect of inclusion into cyclodextrins on the photophysical properties of fluorescent substrates, resulting in emission quenching or enhancement, excimer formation, etc.

Thus complexation of the thermochromic compounds N-5-chloro-salicylideneaniline with cyclodextrins results in the disappearance of the thermochromic property and in the appearance of photochromism. The phenomenon is general e.g. all the thermochromic anils investigated on inclusion to cyclodextrins are transformed to photochromic ones something which might be of interest for various practical applications[18]. The above photo-effects provide incentives for developments in studies of supramolecular photochemistry e.g. to the design of new photoactive molecular devices[17].

SUPRAMOLECULAR CATALYSIS

Supramolecular catalysis, the chemical transformation of the bound substrate, involves first a binding step for which molecular recognition is a prerequisite followed by the transformation of the complexed species and, finally, the release of the product with regeneration of the catalytic unit[19]. A schematic representation of the supramolecular catalysis process is shown in Fig. 7. Thus the macrocyclic polyamine 6 strongly binds ATP and markedly accelerates its hydrolysis to ADP and inorganic phosphate over a wide pH range[20].

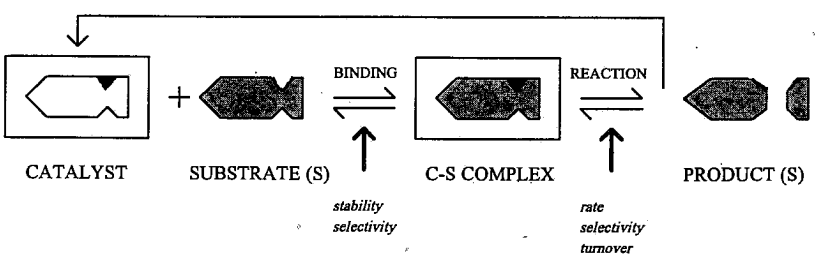

Fig. 7. Schematic representation of the supramolecular catalysis process.

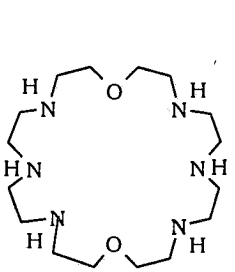

6

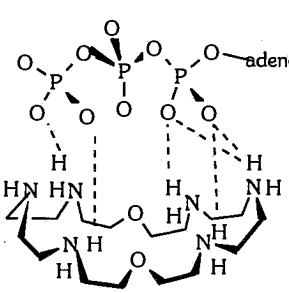

7

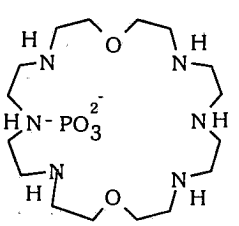

8

The reaction presents first-order kinetics and is catalytic with turnover. It proceeds via initial formation of a complex between ATP and protonated 6, followed by an intracomplex reaction which may involve a combination of acid, electrostatic, and nucleophilic catalysis. Structure 7 represents one possible binding mode of the ATP-6 complex and indicates how cleavage of the terminal phosporyl groups might take place. A transient intermediate identified as phosphoramide 8, is formed by phosphorylation of the macrocycle by ATP and is subsequently hydrolyzed. In this process catalyst 6 presents prototypical ATPase activity, i.e. it behaves as a proto-ATPase. Many other types of supramolecular catalysis may be realised.

Supramolecular catalysts are by nature abiotic reagents, i.e. chemical catalysts that may perform the same overall processes as enzymes, without following the detailed way in which the enzymes actually realize them. This chemistry may develop reagents that effect highly efficient and selective processes that enzymes do not perform or realize enzymatic ones in conditions in which enzymes do not operate[20].

SUPRAMOLECULAR APPLICATIONS AND TECHNOLOGY

Supramolecular chemistry, the chemistry of molecular components and devices, provokes the creative imagination of the chemist to design usefull applications and to contribute in the advancement of technology.

Semiochemistry, the chemistry of molecular signal generation, processing, trasfer, conversion and detection, Supramolecular Devices e.g. structurally organized and functionally integrated chemical systems built into

supramolecular architectures, Programmed Supramolecular Systems e.g. systems that generate organized entities following a defined plan based on molecular recognition events, Chemionics, supramolecular devices that operate on photons, electrons and ions, all are subject to advanced technology and usefull applications [21]. For example a prospective research constitute the applications of cyclotriveratrylenes and cryptophanes to the design of materials for optoelectronics [22].

Excellent prospects exist now also for applications of inclusion compounds to separation problems as for instance those based on cyclodextrins, which are rather new and they hold promise. The molecule, Fig. 4, indicates that the framework is a rigid one. The cavity exists in the solid state in the presence or absence of a guest, and in the liquid state with or without a guest. Significantly, the cavity is of appropriate dimensions to accommodate small hydrocarbon guests as it is shown with 4-tert-butyltoluene and 4-tert-butylbenzoic acid[23,24]. Therefore separation efforts, using cyclodextrins, of xylenes, ethylbenzene, trimethylbenzenes, aldylphenols, straight and branched chain hydrocarbons have been carried out[25].

Cyclodextrins are known to be used also as slow release carriers for many unstable or volatile biologically active substances. Thus they have been used as slow release carriers for the volatile sex attractant pheromone, the 1,7-dioxaspyro[5.5]undecane, in order to control the olive fruit fly, Dacus oleae, a major pest of olives in the Mediterranean region[26].

The outstanding properties of cyclodextrins are used in many different application fields, such as food industry, chemical industry, pharmaceuticals and cosmetics[27].

The future applications, according to the supramolecular system, are therefore numerous ranging from Pimentel's, the late, prediction in 1985 for a manmade molecular scale computer[28,29] to the development of super-conductors[30], biosensors, optical and magnetic materials, enzyme-like catalysis, modern separation science, molecular electronics and other fields based on organization of molecules at the supramolecular level.

ΥΠΕΡΜΟΡΙΑΚΗ ΧΗΜΕΙΑ

Περίληψη: Η υπερμοριακή χημεία αναπτύσσεται ταχύτατα και τα τελευταία χρόνια έχει γίνει τεράστια πρόοδος στον τομέα αυτό. Στο παρών άρθρο, το οποίο δεν είναι δυνατό να καλύψει την ήδη υπάρχουσα τεράστια βιβλιογραφία, παρουσιάζονται ορισμένα τυπικά υπερμοριακά συστήματα κατά τρόπο ώστε να αναδεικνύεται ο δυναμισμός του νέου αυτού πεδίου και να αποτελέσει, ενδεχομένως, αντικείμενο νέων επιστημόνων με δημιουργική φαντασία. Για να επιτευχθεί ο σκοπός αυτός, χωρις τον κίνδυνο του κατακερματισμού, δίνονται συγκεκριμμένα παραδείγματα στην περιοχή του σχεδιασμού και της σύνθεσης, των υπερμοριακών συστημάτων, στη δραστικότητα, στην κατάλυση και τέλος στις εφαρμογές και την τεχνολογία.

REFERENCES

1. Lehn J.-M., Angew. Chem. Int. Ed. Engl. 27, 89 (1988).
2. Fischer E., Chem. Ber. 27, 2985 (1894).
3. Zimmerman S. C., in "Topics in Current Chemistry", Vol. 165, p. 72, Springer-Verlag 1993.
4. Cram D. J., Angew Chem., Int. Ed. Engl. 25, 1039 (1986).
5. Ebmeyer F., Vogtle F., in: "Dugas H (ed) Bioorganic chemistry frontiers", Springer, Berlin Heidelberg, New York, (1991).
6. Kohnke F. N., Mathias J. P. and Stoddart J. F., in: "Topics in Current Chemistry", Vol. 165, p. 3, 1993, and references herein.
7. Cram D. J., in: "Vogtle F, Weber, E (eds) Host guest complex chemistry", Macrocycles, Springer, Berlin Heidelber, New York. p. 125 (1985).
8. Brieanne M. J., Gabard J., Lehn J.-M. and Stibor I., J. Chem. Commun., 1868 (1989); Fourquay C., Lehn J.-M. and Levelut A.-M., Adv. Mater., 2:254 (1990).
9. Sherman J. C. and Cram D. J., J. Am. Chem. Soc., 111, 4527 (1989).
10. Saenger W., Isr. J. Chem., 25, 43 (1985).
11. Mavridis I. M., Hadjoudis E. and Tsoucaris G., Carbohydrate Research, 220, 11 (1991) and references herein.
12. Stoddart F., Chemistry in Britain, 714 (1991).
13. Hoss R. and Vogtle F., Angew. Chem. Int. Ed. Engl., 33, 375 (1994).
14. Amabilino D. B., Ashton P. R., Reder A. S., Spencer N. and Stoddart J. F., Angew. Chem. Int. Ed. Enlg., 33, 1286 (1994).

15. Anelli P. L., Ashton P. R., Ballardini R., Balzani V., Delgado H., Gandolfi M.T., Goodnow T. T., Kaifer A. E., Philp D., Pietra-szkiewicz M., Prodi L., Reddington M. V., Slawin A. M. Z., Spencer N., Stoddart J. F., Vincent C. and Williams D. J., J. Am. Chem. Soc., 114, 193 (1992).

16. Balzani V., Supramolecular Photochemistry, D. Reidel Publishing Co., 1987.

17. Lehn J.-M., in "Supramolecular Photochemistry", Ed. Balzani V., D. Reidel Publishing Co., p. 29, 1987.

18. Pistolis G., Hadjoudis E. and Mavridis I., Mol. Cryst. Liq. Cryst. 242, 215 (1994)

19. Hosseini M. W., La Recherche, 206, 24 (1989).

20. Lehn J.-M., J. Incl. Phenom. 6, 351 (1988).

21. Lehn J.-M., Angew. Chem. Int. Engl. 29 1304 (1990).

22. Collet A., Dutasta J.-P., Lozach B. and Canceil J., in "Supramolecular Chemistry I. Directed Synthesis and Molecular Recognition" Ed. Weber E., Topics in Current Chemistry, V.165, 1993.

23. Mavridis I. and Hadjoudis E., Carbohydrate Research, 229, 1 (1992).

24. Rontoyianni A., Mavridis I., Hadjoudis E. and Duisenberg A., Carbohydrate Research, 252, 19 (1994).

25. Atwood J. L., in "Supramolecular Compounds from Structure to Reactivity" First Int. Summer School of Supramolecular Chemistry, Strasbourg, Sept. 16-28, 1990.

26. Botsi A., Yannakopoulou K. and Hadjoudis E., Carbohydrate Research, 241, 37 (1993).

27. Cyclodextrin and their industrial uses, Ed. Duchene D., Editions de Sante, 1987.

28. Stoddart F., Chemistry in Britain, 714 (August) 1991.

29. Pimentel G. C., Opportunities in Chemistry, p. 220. Washington: National Academy, 1985.

30. Klufers P. and Schuhmacher J., Angew. Chem. Int, Ed. Engl. 33, 1863 (1994).

Chimika Chronika, New Series, 24, 115-132 (1995)

THE USE OF TWO MODELS TO DESCRIBE THE ADSORPTION OF POTASSIUM BY ALFISOLS

A.DIMIRKOU[1], M. DOULA[1] , A.IOANNOU[2]

1. National Agricultural Research Foundation of Greece, Institute of Soil Science, 1 S. Venizelou St. Lycovrissi, 14123, Attiki, Greece.
2. University of Athens, Department of Chemistry, Panepistimiopolis-Zografou, 15771 Attiki, Greece.

(Received October 26, 1993)

SUMMARY

The kinetics of potassium adsorption from solution to exchangeable phases of a soil were investigated on Alfisol Haploxeralf samples, which were firstly saturated with Ca. Potassium adsorption was studied using 5, 25, 100 and 125 μgK/ml solution (or 250, 1250, 5000 and 6250 μgK/g soil) and was equilibrated for (10,20,25,30, 40,45,50,60,80) min and 24 h. Soil pH varied from 4.0 to 9.0. K adsorption equilibrium reached faster at lower initially added K concentrations and higher pH values. Adsorption data was plotted according to first-order kinetic and parabolic diffusion models. Diffusion coefficients were determined and compared. Comparison of regression coefficients (r^2) indicated that the parabolic diffusion model can describe successfully K adsorption.

Keywords : Models , Adsorption , Alfisols.

Postal address of the corresponding author: A.Dimirkou , 14 Thermopillon st. 15344, Pallini, Greece.

INTRODUCTION

Potassium exists in soil systems as diluted in soil solution, exchangeable , nonexchangeable and as a component of minerals. Soil-solution and exchangeable K are considered the readily available forms (Reitemeier,1951). It is believed that K reactions exist between the various forms of K.

The existing reaction between soil solution and exchangeable K has been studied by many researchers . Many of them studied K exchange reactions on pure minerals e.g. bentonite, kaolinite, etc. (Schouwenburg and Scheffelin,1963; Rich and Blach,1964; Goulding and Talibudeen, 1980; Talibudeen and Goulding, 1983; Doula et al., 1994) and on soils (Schwertmann, 1962; Bolt et al., 1963; Singh et al.,1981; Ioannou et al., 1994; Dimirkou et al., 1994). Many investigations on the thermodynamic approach to K exchange equilibrium data have been made (Deist and Talibudeen , 1967). Sparks et al., (1980) studied the kinetics of potassium adsorption from solution to sample exchangeable sites for two Dothan soils. They observed that equilibrium was reached faster when lower initial potassium concentrations were used. Also, the rate of adsorption depended on soil characteristics.

Soils and minerals have a net negative or positive charge. This charge is counterbalanced by opposite charged ions, which are attracted with electrostatic forces on solid phase. At the adsorption process , ions from solution (e.g. K, P etc.) substitute some of counterbalance ions from exchangeable sample sites.

Exchange in pure montmorillonite, "illite" and kaolinite is faster than in vermiculitic materials. This slower rate of exchange in vermiculite is attributed to slow diffusion into interlayers (Malcom and Kennedy,1969) .

The models used to describe potassium exchange are : modified Freundlich equation (Sparks et al.,1980) for potassium adsorption, first-order rate equation for potassium adsorption and desorption (Sparks and Jardine, 1981), Elovich equation for potassium adsorption (Havlin et al., 1985) and parabolic diffusion model for potassium release (Feigenbaum et al.,1981; Havlin and Westfall, 1985) and nth order rate equation (Selim et al.,1976).

The parabolic diffusion model (Jost,1960; Laidler,1965; Sparks,1986) assumes that reaction rate is controlled by the diffusion of ions to the reactive sites, either through a stagnant water film that sourrounds the soil particle, or through the particle itself.

The objectives of the present study were: a) to investigate the influence of pH and initially added K concentration on potassium adsorption by Alfisol Haploxeralf soils and b) to determine which of the tested models (First-order kinetic and parabolic diffusion) fits experimental data best.

MATERIALS AND METHODS

Studies were performed on a soil sample from central Greece (Viotia). Sample taxonomic classification, and physical and chemical properties are given in Table I. The soil sample was air-dried and crushed to pass a 2-mm sieve. Particle size analysis was determined by the pipette method (Kilmer and Alexander, 1949). Organic matter was determined by the Walkley-Black (1934) method.Cation exchange capacity by a $MgCl_2$ saturation with subsequent displacement by $CaCl_2$ (Okazaki et al., 1963; Rich ,1962). The exchangeable K was determined following extraction by 1N ammonium acetate. The electrical conductivity (E.C.) was measured in a saturated paste of the soil.The pH measurements was obtained from a 1:2 soil/water mixture. The $CaCO_3$ equivalent was determined by treatment with dilute acid and the volume of released CO_2 measured by the Bernard Calcimeter.

Sample preparation

Before the beggining of the kinetic adsorption studies , soil sample was Ca-saturated using 1N $CaCl_2$. The soil was subsequently washed with deionized water followed by 1:1 acetone-H_2O mixture until a negative test for Cl^- was obtained with $AgNO_3$. The soil was saturated with Ca as, in most mineral soils, this is one of the predominate cation. Also, by saturating with this Ca^{+2}, the most of exchangeable K was removed from the soils. The saturated sample was air-dried and crushed to pass a 2-mm sieve. Soil pH was measured on Ca-saturated samples using 1:2 soil/water solution. The C.E.C. (Cation Exchange Capacity) of Ca-saturated samples was ascertained by displacement with 1N $MgCl_2$. The quantity of Ca in solution was measured using atomic absorption spectrophotometry.

TABLE I : Soil physical and chemical characteristics

Depth cm	Sand %	Silt %	Clay %	Liquid limit
0-50	16	14	70	68
EC mmhos/cm	**pH 1:2**	**C.E.C. meq/100g**	**Organic matter %**	**Exchangeable K , meq/100g**
<3	7.8	42	0.8	0.80
C.E.C. after Ca-saturation	**pH after Ca-saturation**			
48.25	7.1			

Kinetics of adsorption

Adsorption studies were carried out using triplicate 1-gram Ca-saturated sample which were placed in 100 ml polypropylene centrifuge tubes with 50 ml of 5, 25, 100 and 125 μgK/ml solution and 20 ml of buffer solution pH 4.0, 5.0, 7.0, 8.0, 9.0. After equilibration at 25°C for 10, 20, 25, 30, 40, 45, 50, 60, 80 min and 24 h, the suspensions were centrifuged and K determined in the liquid phase.The amount of K sorbed was calculated by subtracting the final from the initial potassium concentration. Concentration differences before and after shaking were assumed to represent the amount of K that sorbed on soil material surfaces.

Two mathematical models used to describe potassium sorption process by Alfisol Haploxeralf soils, are first-order kinetic model and parabolic diffusion model.

Considering that the adsorption process follows the first order rate law and that before equilibrium K desorption is negligible ($k_{des} << 1$) , the following equations can be written:

$$K_{solution} \xrightarrow{k_{ad}} K_{soil}$$

$$-\frac{dC_{solution}}{dt} = k_{ad} C_{solution} \Leftrightarrow -\frac{d(C_o - X)}{C_o - X} = k_{ad} t$$

$$\Leftrightarrow -\frac{d(C_o - X)}{C_o - X} = k_{ad} t \Leftrightarrow -\ln(C_o - X) + \ln C_o = k_{ad} t$$

$$\Leftrightarrow \ln(C_o - X) = \ln C_o - k_{ad}t \Leftrightarrow \ln C = \ln C_o - k_{ad}t \qquad (1)$$

where C (μgK/g soil) is the potassium concentration in soil solution at reaction time t (sec), C_o (μgK/g soil) is the initial potassium concentration, X (μgK/g soil) is the amount of K sorbed per unit weight of soil and k (sec^{-1}) is the reaction rate coefficient. By plotting lnC versus t a straight line is obtained with slope equal to k and intersept equal to $\ln C_o$.

Many researchers have used the first order kinetic model in the following form : lnX=a-bt (2) (Havlin and Westfall, 1985). Equation (2) is not in agreement with the arised equation (1) . Nevertheless, both forms of the first order model were tested on experimental data.

The parabolic diffusion model used in this study is:

$$Xt=c+Rt^{1/2} \qquad (3)$$

where X_t (μgK/g soil) is the amount of K adsorbed at time t , t (sec) is the reaction time, R is a transport term proportional to the diffusion constant. The parabolic rate equation allows to calculate only an overall diffusion constant (R). By using the model proposed by Chute and Quirk (1967) it is possible to form a view for process diffusion coefficient. This model based on radical diffusion in a cylinder in which the concentration of potassium on the cylinder surface is constant and the concentration of potassium throughout the cylinder is initially uniform. It is assumed that the diffusion through the upper and lower faces of the cylinder (Corresponding the external cleavage faces) is negligible. Radial diffusion equation is simplified by Chute and Quirk (1967) and has the form :

$$\frac{X_t}{X_\infty}\frac{1}{t} = \frac{4}{\sqrt{\pi}}\left(\frac{D}{a^2}\right)^{0.5} t^{-0.5} - \left(\frac{D}{a^2}\right) \qquad (4)$$

where X_t (μgK/g soil) is K quantity which had entered into the cylinder in time t, X_∞ (μgK/g soil) is the corresponding K quantity after an infinite time, D is the diffusion coefficient and a is the radius of the cylinder. By plotting $\frac{X_t}{X_\infty}\frac{1}{t}$ versus $t^{-0,5}$ a straight line should be obtained with slope equal to $\frac{4}{\sqrt{\pi}}\left(\frac{D}{a^2}\right)^{0.5}$.

RESULTS AND DISCUSSION.

The different behaviour of K adsorption is owed to different pH values and different potassium concentrations. As shown in Figure 1 (using, as example ,one of tested concentrations) pH is a significant factor that influences K sorption. Altough not shown the same behaviour appeared to all tested initial concentrations. An increase in pH caused faster and higher K sorption due to the formation of new sorption sites (-Si-OH $\leftrightarrow$ -Si-O^- + H^+), and to the decrease of competition between H^+ and K^+ for those sites.

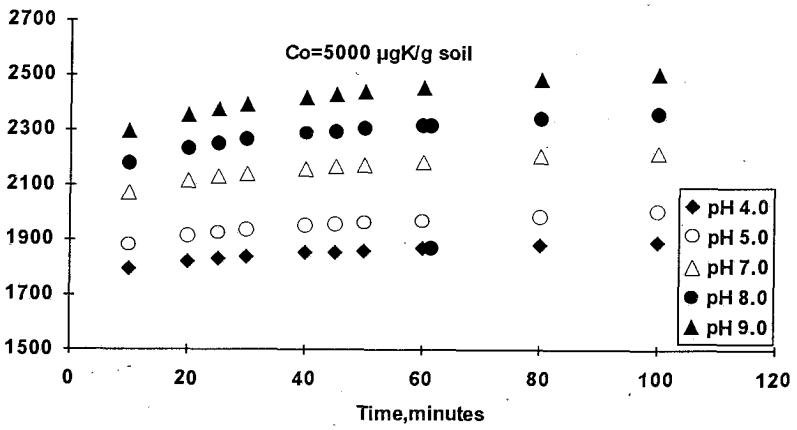

Fig. 1. *POTASSIUM SORPTION BY ALFISOL HAPLOXERALF FOR Co=5000µgK/g SOIL FOR pH VALUES 4.0 , 5.0 , 7.0 , 8.0 AND 9.0*

These results are in agreement with those of Garcia-Miragaya and Page (1987).

When higher potassium concentrations are used the potassium exchange rate decreases.This can be explained by the increase in total positive potential on the surface due to potassium adsorption and increased interaction between adsorbate species. An example for pH 8.0 is shown in Figure 2.

The first-order kinetic model was tested to all pH values and all initial K concentrations. Figure 3 shows, the first order model fitted to K concentration 100 ppm to all pH values.

The calculated values of slopes (b) , intersepts (a) and linear coefficients (r^2) are summarized in Table II. For the same initial K concentration and for all tested pH values

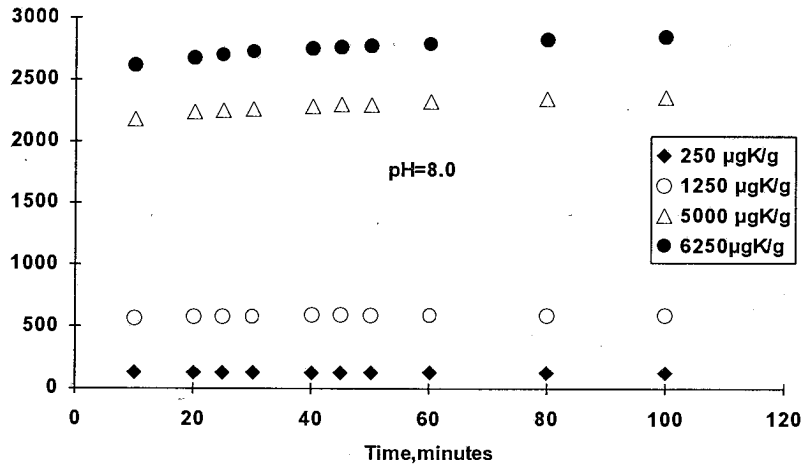

Fig.2. *POTASSIUM SORPTION BY ALFISOL HAPLOXERALF FOR pH 8.0 AND FOR INITIAL CONCENTRATIONS 250, 1250, 5000 AND 6250 µgK/g SOIL .*

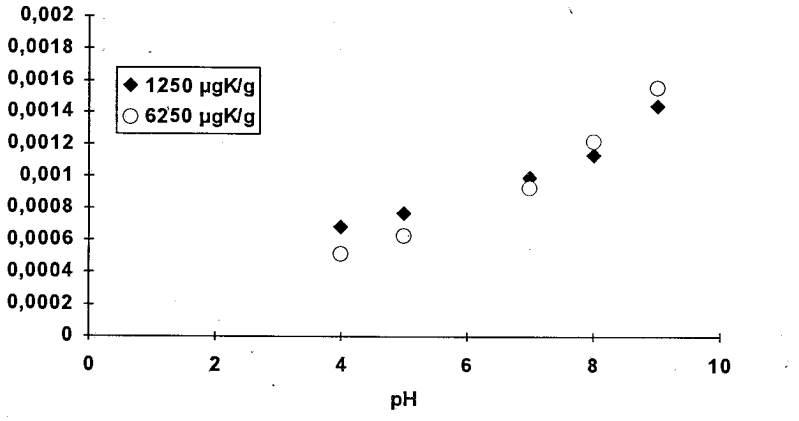

Fig. 3. *FIRST ORDER RATE MODEL FOR POTASSIUM SORPTION BY ALFISOL HAPLOXERALF FOR Co=5000 µgK/g SOIL AND FOR pH VALUES 4.0, 5.0, 7.0, 8.0 AND 9.0*

the intersepts must be constant and equal to lnCo. Nevertheless, the calculated intersepts are lower than lnCo and they depend upon the sample pH value.

Concidering that a=f lnCo ⇔ f=a/lnCo , it is possible to calculate the coefficient f which the second part of equation (1) is multiplied. It was also assumed that the slopes of regression equations are multiplied with the same coefficient f : b=f k ⇔ k=b/f (5), where k is the reaction rate coefficient.

The calculated values of f and k (Table II) are presented as function of pH in Figures 4, 5 and 6. Reggression coefficients of those lines indicate that the regression equations for k and f may be used in order to arise a pH-depended form of first order model (Table III).

The model which is usually described as the first-order model in literature is:

$$\ln X = a - bt \quad (6)$$

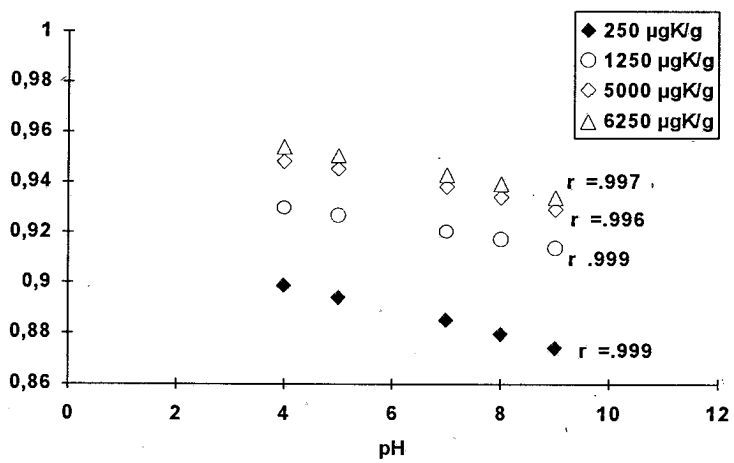

Fig. 4. *VALUES OF COEFFICIENT f AS FUNCTION OF pH FOR INITIAL CONCENTRATIONS 250, 1250, 5000 AND 6250 µgK/g SOIL.*

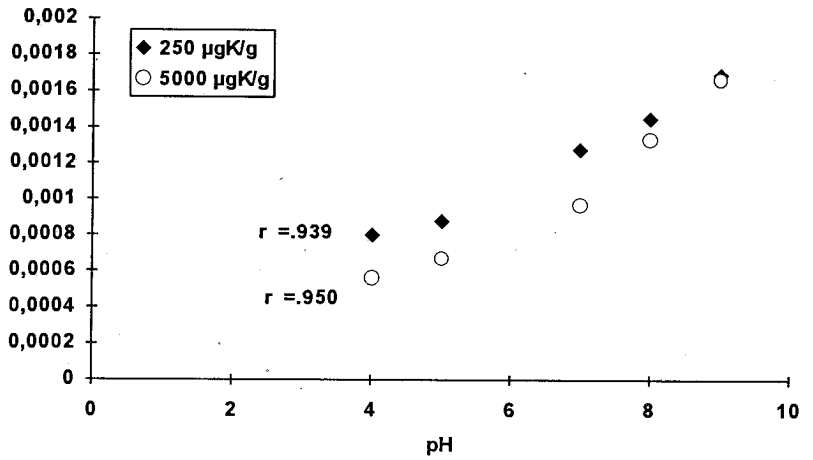

Fig. 5. *VALUES OF RATE COEFFICIENT k AS FUNCTION OF pH FOR INITIAL CONCENTRATIONS VALUES 250 AND 5000 µgK/g SOIL.*

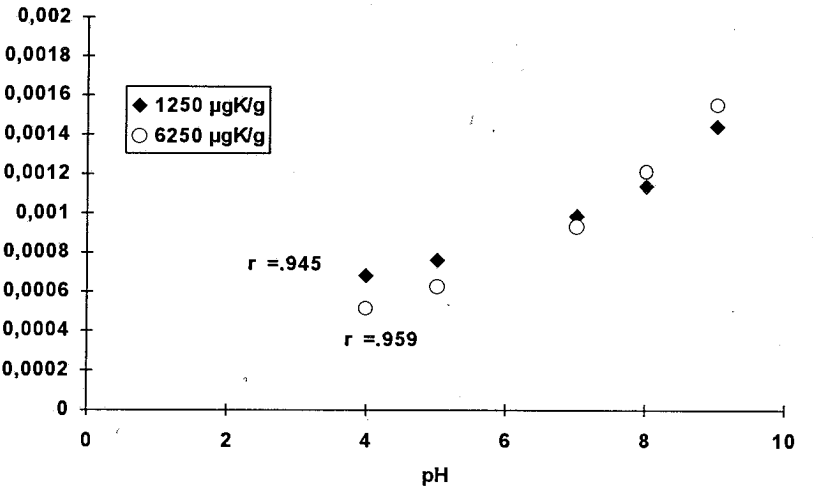

Fig. 6. *VALUES OF RATE COEFFICIENT k AS FUNCTION OF pH FOR INITIAL CONCENTRATIONS 1250 AND 6250 µgK/g SOIL.*

TABLE II : Values of slopes (a) , intersepts (b) , coefficients f , rate coefficients (k) and linear coefficients (r^2) for the first order rate model.

250 µgK/g	a	b	r^2	f	k
pH 4.0	4.963	-7.9×10^{-4}	0.949	0.8989	8.02×10^{-4}
pH 5.0	4.936	-7.17×10^{-4}	0.942	0.8940	8.79×10^{-4}
pH 7.0	4.885	-1.13×10^{-3}	0.960	0.8847	1.28×10^{-3}
pH 8.0	4.856	-1.28×10^{-3}	0.960	0.8794	1.46×10^{-3}
pH 9.0	4.826	-1.48×10^{-3}	0.958	0.8740	1.69×10^{-3}
1250 µgK/g	**a**	**b**	**r^2**	**f**	**k**
pH 4.0	6.631	-6.32×10^{-4}	0.949	0.9299	6.80×10^{-4}
pH 5.0	6.609	-7.10×10^{-4}	0.944	0.9268	7.66×10^{-4}
pH 7.0	6.562	-9.12×10^{-4}	0.950	0.9202	9.91×10^{-4}
pH 8.0	6.538	-1.04×10^{-3}	0.949	0.9169	1.14×10^{-3}
pH 9.0	6.516	-1.32×10^{-3}	0.961	0.9137	1.45×10^{-3}
5000 µgK/g	**a**	**b**	**r^2**	**f**	**k**
pH 4.0	8.075	-5.30×10^{-4}	0.945	0.9481	5.59×10^{-4}
pH 5.0	8.048	-6.32×10^{-4}	0.949	0.9449	6.69×10^{-4}
pH 7.0	7.987	-9.12×10^{-4}	0.950	0.9378	9.73×10^{-4}
pH 8.0	7.953	-1.25×10^{-3}	0.951	0.9338	1.34×10^{-3}
pH 9.0	7.914	-1.55×10^{-3}	0.959	0.9292	1.67×10^{-3}
6250 µgK/g	**a**	**b**	**r^2**	**f**	**k**
pH 4.0	8.339	-4.92×10^{-4}	0.972	0.9541	5.16×10^{-4}
pH 5.0	8.309	-6.00×10^{-4}	0.952	0.9506	6.31×10^{-4}
pH 7.0	8.242	-8.80×10^{-4}	0.958	0.9430	9.33×10^{-4}
pH 8.0	8.206	-1.14×10^{-3}	0.952	0.9389	1.22×10^{-3}
pH 9.0	8.163	-1.45×10^{-3}	0.956	0.9339	1.56×10^{-3}

The first order model (equation 2) was tested on experimental data and was found to describe the sorption succesfully. The values of intersepts (a), slopes (b) and regression coefficients (r^2) for all the experimental conditions presented in Table IV.

TABLE III : pH - depended forms of first order model for all initial concentrations

Co µgK/g	pH depended forms of first order model lnC=f (lnCo-kt)
250	$\ln C = (0.919-4.94\times10^{-3}pH)\ [\ \ln Co-(5.29\times10^{-5}+1.77\times10^{-4}pH)\ t\ ]$
1250	$\ln C = (0.943-3.26\times10^{-3}pH)\ [\ \ln Co-(5.77\times10^{-5}+1.43\times10^{-4}pH)\ t\ ]$
5000	$\ln C = (0.964-3.74\times10^{-3}pH)\ [\ \ln Co-(-3.95\times10^{-4}+2.18\times10^{-4}pH)\ t\ ]$
6250	$\ln C = (0.970-3.99\times10^{-3}pH)\ [\ \ln Co-(-3.57\times10^{-4}+2.01\times10^{-4}pH)\ t\ ]$

Authors concidered this model as an empirical one which can provide a good description of adsorption process. The values of characteristic constants a and b increase as pH and initial concentrations increase.

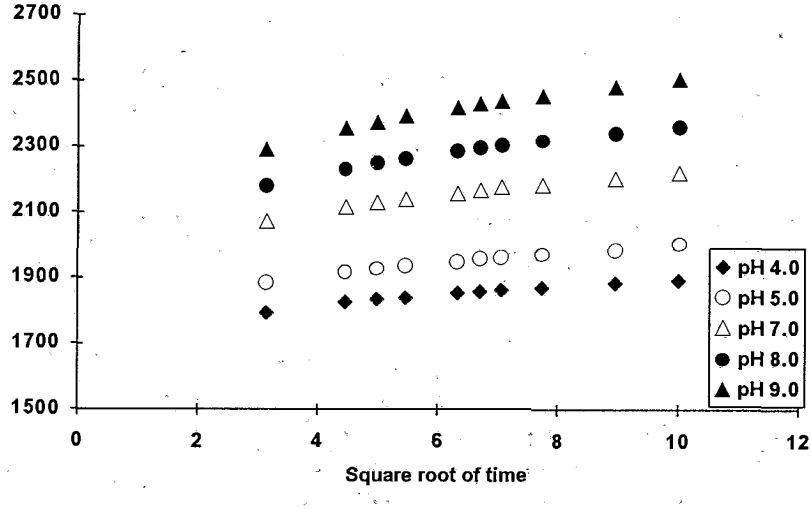

Fig. 7. *PARABOLIC DIFFUSION MODEL FOR POTASSIUM SORPTION BY ALFISOL HAPLOXERALF FOR Co 5000 µgK/g SOIL AND FOR pH VALUES 4.0, 5.0, 7.0, 8.0 AND 9.0*

The parabolic diffusion model is the model which describes K sorption better than the other two. Plots of X_t vs square root of time give a nonlinear relationship due to sorption of K on the external planer surface sites, suggested that film diffusion was the rate-controlling rate. Figures (7) and (8) present the parabolic diffusion model for Co 5000 μgK/g and all pH values and for pH 8.0 and all initial concentrations, respectively.

By using equation (3) linear plots were obtained (Fig. 9, 10) . The calculated slopes of those lines are analogous to diffusion coefficients (Table V).

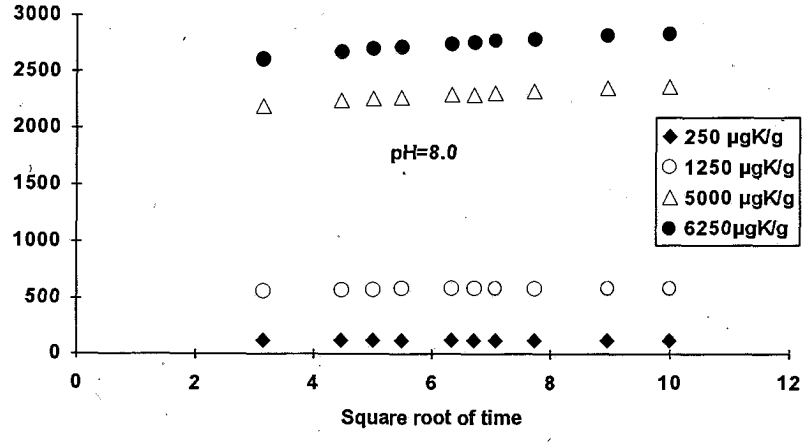

Fig. 8. *PARABOLIC DIFFUSION MODEL FOR POTASSIUM SORPTION BY ALFISOL HAPLOXERALF FOR pH VALUE 8.0 AND FOR INITIAL CONCENTRATIONS 250, 1250, 5000 AND 6250 μgK/g SOIL*

The diffusion coefficient D decreases with the increase in the initial K concentration. As the number of K^+ ions increases , a saturation of external surface sites occured and this fact resulted in a decrease of diffusion coefficient.

For the same initial concentration, the diffusion coefficient increases with increasing pH, although at pH 4.0 appears an increase compared to pH 5.0.

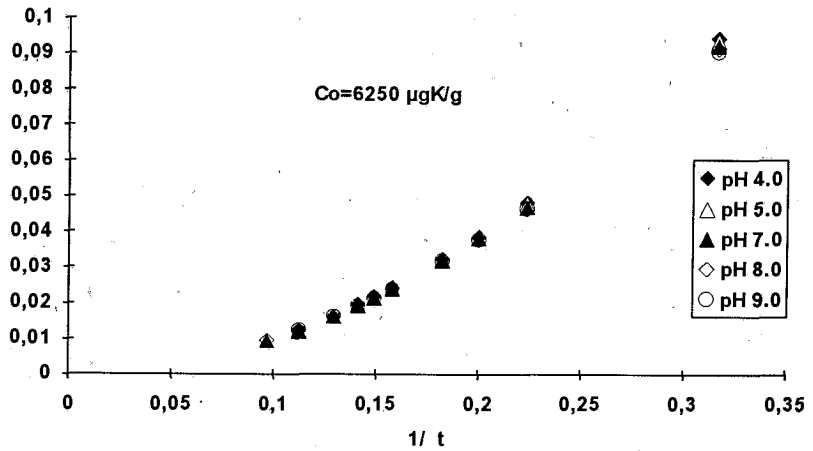

Fig. 9. *PLOTS OF Xt/X_∞ AS FUNCTION OF 1/ t FOR Co=6250 µgK/g SOIL AND FOR pH VALUES 4.0, 5.0, 7.0, 8.0 AND 9.0.*

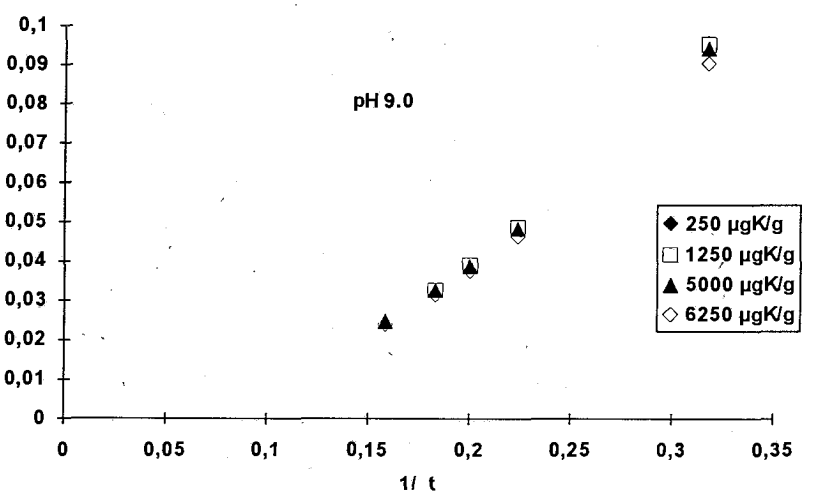

Fig. 10. *PLOTS OF Xt/X_∞ AS FUNCTION OF 1/ t pH FOR pH VALUE 9.0 AND FOR INITIAL CONCENTRATIONS 250, 1250, 5000 AND 6250 µgK/g SOIL.*

At strong acidic conditions (pH 4.0) a decomposition of clay takes place, resulted in K, Al, Mg. and Fe release (Feigenbaum et al., 1981). The mobility of those ions and the competition between them in order to occupy the sorption sites resulted in an increase of diffusion coefficient.

In alkaline soil solution diffusion coefficients increase because the clay is negative charged, the sorption intensity is great and occured also to internal surfaces.

TABLE IV : Values of slopes (a), intersepts (b) and linear coefficients (r^2) for the kinetic model lnX=a-bt

Co=250μgK/g	**pH 4.0**	**pH 5.0**	**pH 7.0**	**pH 8.0**	**pH 9.0**
a	4.675	4.705	4.769	4.803	4.832
b	$9.34x10^{-4}$	$9.76x10^{-4}$	$1.19x10^{-3}$	$1.15x10^{-3}$	$1.35x10^{-3}$
r^2	0.942	0.953	0.948	0.945	0.955
Co=1250μgK/g	pH 4.0	pH 5.0	pH 7.0	pH 8.0	pH 9.0
a	6.199	6.231	6.296	6.327	6.353
b	$9.46x10^{-4}$	$1.01x10^{-3}$	$1.12x10^{-3}$	$1.21x10^{-3}$	$1.48x10^{-3}$
r^2	0.948	0.950	0.946	0.943	0.953
Co=5000μgK/g	**pH 4.0**	**pH 5.0**	**pH 7.0**	**pH 8.0**	**pH 9.0**
a	7.488	7.535	7.629	7.680	7.725
b	$9.34x10^{-4}$	$1.04x10^{-3}$	$1.25x10^{-3}$	$1.39x10^{-3}$	$1.75x10^{-3}$
r^2	0.942	0.946	0.948	0.945	0.953
Co=6250μgK/g	**pH 4.0**	**pH 5.0**	**pH 7.0**	**pH 8.0**	**pH 9.0**
a	7.634	7.693	7.805	7.860	7.919
b	$9.56x10^{-4}$	$1.07x10^{-3}$	$1.30x10^{-3}$	$1.51x10^{-3}$	$1.70x10^{-3}$
r^2	0.946	0.942	0.933	0.946	0.939

TABLE V : Values of slopes (b) and linear coefficients (r^2) for the plots of Xt/X_∞ vs 1/ t (parabolic diffusion model)

Co=250µgK/g	pH 4.0	pH 5.0	pH 7.0	pH 8.0	pH 9.0
b	0.4334	0.4180	0.4800	0.4560	0.4780
r^2	0.987	0.985	0.997	0.992	0.997
Co=1250µgK/g	pH 4.0	pH 5.0	pH 7.0	pH 8.0	pH 9.0
b	0.4330	0.4170	0.4560	0.4540	0.4750
r^2	0.987	0.985	0.992	0.992	0.997
Co=5000µgK/g	pH 4.0	pH 5.0	pH 7.0	pH 8.0	pH 9.0
b	0.4186	0.3780	0.4260	0.4230	0.4470
r^2	0.984	0.967	0.988	0.988	0.992
Co=6250µgK/g	pH 4.0	pH 5.0	pH 7.0	pH 8.0	pH 9.0
b	0.4013	0.3810	0.3750	0.3710	0.3830
r^2	0.979	0.973	0.973	0.974	0.981

CONCLUSIONS

1. An increase in pH cuses faster and higher K sorption.
2. From the tested models, parabolic diffusion model is found to describe the K sorption succesfully.
3. The diffusion coefficient D increases as the initial K concentration and pH increase.

ΧΡΗΣΗ ΔΥΟ ΜΑΘΗΜΑΤΙΚΩΝ ΜΟΝΤΕΛΩΝ ΓΙΑ ΤΗΝ ΜΕΛΕΤΗ ΤΗΣ ΠΡΟΣΡΟΦΗΣΗΣ ΤΟΥ ΚΑΛΙΟΥ ΑΠΟ ΕΔΑΦΗ ΤΥΠΟΥ ALFISOL.

ΠΕΡΙΛΗΨΗ

Στην εργασία αυτή γίνεται μελέτη της κινητικής της προσρόφησης του καλίου σε εδάφη τύπου Alfisol. Στα εδαφικά δείγματα, μετά από κορεσμό που υπέστησαν με Ca ($CaCl_2$) προστέθηκε κάλιο (KCl) σε συγκεντρώσεις 250, 1250, 5000, 6250 μgK/g εδάφους και τα συστήματα αφέθηκαν σε επαφή για 10,20,25,30,40,45,50,60,80 λεπτά και 24 ώρες Το pH του εδαφικού διαλύματος κυμαίνονταν από 4.0 έως 9.0.
Παρατηρήθηκε ότι η αντίδραση προσρόφησης και η τελική ισορροπία σε χαμηλές αρχικές συγκεντρώσεις και υψηλό pH ήταν γρηγορες.
Για την εξήγηση των πειραματικών αποτελεσμάτων χρησιμοποιήθηκαν δύο μοντέλα για την κινητική πρώτης τάξης και το μοντέλο διάχυσης. . Το μοντέλο που περιγράφει το φαινόμενο καλύτερα είναι αυτό της διάχυσης (μεγαλύτερο r^2).Οι συντελεστές διάχυσης προσδιορίσθηκαν και συγκρίθηκαν

REFERENCES

1. Bolt,G.H., M.E.Summer, and A.Kamphorst. "A study of the equilibria between three categories of potassium in an illitic soil". *Soil Sci.Soc.Am.Proc.* **27**:294 (1963)
2. Chute,J.H. and Quirk,J.P.,". Diffusion of potassium from mica-like minerals".*Nature,* London, **213** : 1156 (1967)
3. Dimirkou A.,A.Ioannou, J.Mitsios,Ch.Deligianni." Kinetics of potassium adsorption by Entisols of Greece " Commun. Soil Sci. Plant Anal. **25 :** 1417 (1994).
4. Doula M., A.Ioannou, A.Dimirkou, J.Mitsios. " Potassium sorption by Calcium-Bentonite (Ca-b) " Commun. Soil Sci. & Plant Anal. **25 :** 1387. (1994)
5. Deist,J.,and Talibudeen. "Thermodynamics of K-Ca exchange in soils". *J.Soil Sci.* **18**:138 (1967).
6. Feigenbaum,S., R.Edelstein, and I.Shainberg. ." Release rate of potassium and structural cations from micas to ion exchangers in dilute solutions". *Soil Sci.Soc.Am.J.* **45**:501 (1981).
7. Garcia-Miragaya, J., and Page, A.L.. "Influence of ionic strength and inorganic complex formation on the sorption of trace amounts of Cd by montmorillonite." Soil Science Society of America Journal **40** : 658 (1976).
8. Goulding, K. W. T., and O. Talibudeen. "Heterogeneity of cation exchange sites for K-Ca exchange in aluminosilicates." *J.Colloid Interface Sci.* **78**:15 (1980)
9. Havlin,J.L., and D.G. Westfall. "Potassium release kinetics and plant response in calcareous soils". *Soil Sci.Soc.Am.J.* **49**:366 (1985).
10. Havlin,J.L., D.G.Westfall , and R.S.Olsen. "Mathematical models for potassium release kinetics in calcareous soils." *Soil Sci.Soc.Am.J.***9**:371 (1985)
11. Ioannou A.,A.Dimirkou, J.Mitsios, M.Doula. "Kinetics of potassium adsorption by Alfisols of Greece." Commun. Soil Sci. Plant Anal. **25 :** 1401 (1994).
12. Jost,W. "Diffusion in solids,liquids,gases" .Academic Press, N.Y. (1960).
13. Kilmer,V.J., and L.T. Alexander.. "Methods of making mechanical analyses of soils". *Soil Sci.* **68**:15 (1949).
14. Laidler,K.J. "Chemical kinetics".McGraw-Hill Booh Co.,N.Y. (1965)
15. Malcom R. L., and V. C. Kennedy." Rate of cation exchange on clay minerals as determined by specific-ion electrode techniques." *Soil Sci.Soc.Am.Proc.* **33**:247 (1969)
16. Okazaki,R., H.W. Smith, and C.D. Moodie.." Hydrolysis and salt-retention errors in conventional cation exchange capacity procedures". *Soil Sci.* **96**:205 (1963)
17. Reitemeier R. F. "The chemistry of soil potassium "*Adv.Agron.* **3**:113 (1951).
18. Rich, C.I., and W.R.Black. "Potassium exchange as affected by cation size,pH, and mineral structure." *Soil Sci.* **97**:384 (1964)
19. Rich, C.I. "Removal of excess salt in cation-exchange capacity determinations." *Soil Sci.* **93**:87 (1962)
20. Selim, H. M., R. S. Mansell, and L. W. Zelazny. " Modeling reactions and transport of potassium in soils." *Soil Sci.* **122**:77 (1976).
21. Singh, D., R. Pal, and S. R. Poonia. "Exchange equilibria of potassium versus calcium plus magnesium in soils of arid and semiarid region, India "

. *Geoderma* **25**:55 (1981)
22. Sparks, D.L., and P.M. Jardine . "Thermodynamics of potassium exchange in soil using a kinetics approach. " *Soil Sci.Soc.Am.J.* **45**:1094 (1981).
23. Sparks, D.L., L.W.Zelazny, and D.C.Martens."Kinetics of potassium exchange in a Paleudult from the Coastal Plain of Virginia." *Soil Sci.Soc.Am.J.* **44**:37 (1980)
24. Sparks , D.L., D.C. Martens, and L.W.Zelazny . "Plant uptake and leaching of applied and indigenous potassium in Dothan soils." *Agron.J.* **72**:551 (1980).
25. Schouwenburg,J.Ch, and A.C. Schuffelin."Potassium behaviour of an illite. *Neth.J.Agric.Sci.* **11**:13 (1963)
26. Schwertmann,U., "Die selektive kationensorption der tonfraktion einger boden aus sedimenten." *Z.Pflanzenernaehr. Dung Bodenkd.* **97**:9 (1962)
27. Talibudeen, O., and K.W.T. Goulding "Charge heterogeneity in the smectities" *Clays Clay Miner.* **31**:37 (1983).
28. Walkley, A.,and T.A.Black. "An examination of the Degtjareff method for determination soil organic matter and a proposed modification of the chromic acid titration method. " *Soil Sci.***37**:29 (1934).

Chimika Chronika, New Series, 24, 133-146 (1995)

OLIGONUCLEAR ZINC(II) COMPLEXES OF DIANIONS OF HYDROCAFFEIC, CAFFEIC AND FERULIC ACIDS

A.L. PETROU[1]* and S.P.PERLEPES[2]

1. Laboratory of Inorganic Chemistry, University of Athens, Panepistimiopolis, Kouponia, Athens 15701, Greece

2. Department of Chemistry, University of Patras, Patras, Greece

(Received December 14,1993)

SUMMARY

Oligomeric complexes of zinc(II) with the dianions of hydrocaffeic, caffeic and ferulic acids in methanol : water 9:1 solutions were prepared and studied. They are given the empirical formulae : $K_2[Zn_3(hydcafH)_3(OH)_2].2H_2O.MeOH$, $K[Zn_3(cafH)_3(OH)(H_2O)_2].H_2O.2MeOH$ and $K[Zn_3(fer)_3(OH)(H_2O)_2].H_2O.MeOH$. The simultaneous zinc(II) ion coordination to both carboxylic and catecholic sites ,which leads to the formation of tetrahedral oligomeric species with ligand to zinc molar ratio of 1:1, is supported by spectroscopic (i.r., far-i.r., n.m.r.), thermogravimetric and potentiometric data , elemental analyses and conductivity measurements.

Key words : hydrocaffeic acid ,caffeic acid, ferulic acid, oligonuclear zinc(II) complexes

INTRODUCTION

Zinc(II) is essential for the normal function of most organisms , as has been extensively documented by nutritional work over several years [1] .It has been implicated as a cofactor required for a variety of biochemical processes in plants, bacteria and higher organisms [1].Several metabolically important reactions are catalyzed by zinc(II) enzymes including hydrolysis,

* Author to whom correspondence should be addressed.

hydration and group-transfer reactions. This role of zinc(II) in the catalytic mechanism of a number of enzymes is its function as a Lewis acid withdrawing electrons from a group of the substrate directly coordinated to the metal ion at a site initially occupied by solvent water. In carbonic anhydrase the Zn(II)-bound water at the active center deprotonates to yield the good nucleophile Zn(II)-OH^- which attacks the electrophilic center of the substrate CO_2 . Zinc(II) may also function by maintaining the required conformation of a protein or by participating in the binding of effector molecules to allosteric enzymes. For example, the Zn(II) ion of equine alcohol dehydrogenase is bonded to four cysteines, as is the case for zinc in the regulatory subunit of aspartate carbamoyltransferase. In the linear sequence these cysteines are close to one another, separated by 2,2 and 7 or 4, 22 and 2 amino acids, respectively. For both systems the zinc is tetrahedrally coordinated to the four cysteines, preventing access of water or substrate to its coordination sphere; the role of Zn(II) apparently is to maintain the structure of the protein in its immediate vicinity. Another important biological role for zinc has recently began to emerge. Zn(II) has been shown to be an effective inhibitor of renin and HIV-1 protease, a finding that could help to explain some of the beneficial effects seen in AIDS patients who have received Zn(II) therapy.

The bioavailability to plants of metal ions is greatly influenced by coordinating ligands which may be present in the soil or in the synthetic nutrient solutions in which the plants grow[2]. It is important thus to understand the role of complexation in the uptake of metals by plants. Of special interest are phenolic compounds. The most important of these phenolic compounds are 3,4-dihydroxyphenylpropionic acid (dihydrocaffeic acid, hydcafH_3) **1**, trans-3-(3,4-dihydroxyphenyl)-

propenoic acid (caffeic acid, $cafH_3$)[3] 2 and 3-(4-hydroxy-3-methoxy-phenyl)-propenoic acid (ferulic acid, $ferH_2$) 3.

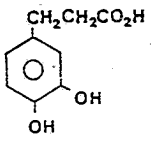

1

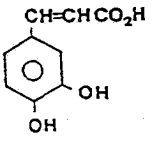

2

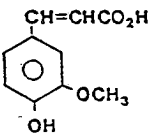

3

Caffeic acid can form complexes with various metal ions that occur in nutrient and soil solutions. Hydrocaffeic acid was recognized as a catechol metabolite of caffeic acid, which can also be produced by human intestinal bacteria [4]. The goal of this paper was to prepare zinc(II) complexes of hydrocaffeic, caffeic and ferulic acids and to study their structures and properties, contributing thus in the understanding of the role of complexation in the uptake of metals by plants.

EXPERIMENTAL

(i) Materials : Hydrocaffeic acid was obtained from Fluka A.G., and caffeic acid and ferulic acid were obtained from Merck. Their purity was checked by mass spectra : m/e of the molecular ions 182 (calcd. 182.2), 180 (calcd. 180.2), 194(calcd. 194.2) for hydrocaffeic, caffeic and ferulic acids, respectively. Details for the preparation and characterization of their sodium salts $hydcafH_2Na.H_2O$, $cafH_2Na.H_2O$ and $ferHNa.H_2O$ have been given in a previous work [5].

(ii) Methods : The Zn contents were determined after titration with EDTA using Eriochrome Black T as indicator [6]. The K contents were determined with potassium ion-selective electrodes. Elemental analyses, physicochemical and spectroscopic measurements were carried out by published methods [7].

(iii) Preparation of the complexes : For the preparation of the complexes , to a solution of hydcafH_3, cafH_3 or ferH_2 (0.01 mole, 0.5M) in MeOH a solution of KOH (0.01 mole , 0.5M) in MeOH was added dropwise with stirring and to the clear solutions so obtained, a solution of $ZnCl_2$ (0.005 mole, 0.25M) in MeOH was gradually added, until a final ratio of Zn:acid ligand :KOH of 1:2:2 was obtained. A light brown solution with a white solid resulted in the case of hydcafH_3, an amount of deep gray solid in the case of cafH_3, and a light beige solid in the case of ferH_2. The prepared complexes were filtered off, washed with MeOH and dried over P_4O_{10} for several days.

RESULTS AND DISCUSSION

Elemental analyses, yields, colours and molar conductivities of the three complexes are reported in TABLE I. The Λ_M values of complex **6** in DMSO and MeOH are in accord with this compound being formulated as an 1 : 1 electrolyte [8]. The values for complexes **4** and **5** are anomalous on the basis of the structures proposed in the solid state (see below).Several explanations can be given for this fact , i.e. ion-pairing in solution , re-organization of the complexes in solution , several species in equilibrium etc., but all are speculative. The complexes were also studied by thermal (t.g./d.t.g.).For complex **4** , the measurements are consistent with a methanol release occuring between 30-60 ^{0} C (3.5% of the sample weight) and a water release occuring in a second step. In the first step (60-70 ^{0}C) 3.9 % of the sample weight is lost and in the second step (70-90 ^{0}C) approximately 2% of the sample weight is removed.For complex **5**, methanol release occurs in a first step at 50-80 ^{0}C (7% of the sample weight) and in a second step at 80-160 ^{0}C water is removed from the sample (6% of its weight). For complex **6** , methanol is removed at 50-70 ^{0}C (3.5% of the sample weight) and water in two different steps. In the

TABLE I.Preparative data, elemental analyses and conductivities of the complexes.

Compound	Complex	Yield [a] (%)	Colour	Found (Calcd.) % Zn	K	C	H	Λ_M [b] ($S\ cm^2\ mol^{-1}$) DMSO	MeOH
4	$K_2[Zn_3(hydcafH)_3(OH)_2].2H_2O.MeOH$	40	light broun	20.7(21.4)	9.2(8.5)	35.9(36.7)	2.98(3.71)	25	90
5	$K[Zn_3(cafH)_3(OH)(H_2O)_2].H_2O.2MeOH$	30	deep gray	22.3(21.7)	3.9(4.3)	37.8(38.5)	3.26(3.65)	6	63
6	$K[Zn_3(fer)_3(OH)(H_2O)_2].H_2O.MeOH$	45	light beige	22.1(21.5)	5.0(4.3)	40.4(40.7)	3.56(3.83)	47	152

[a] Based on the metal. [b] Molar conductivities for ca. 10^{-3} M solutions.

first step (70-220 ^{0}C) approximately 3.9% of the sample weight is released while in the second step (220-270 ^{0}C) 2.0% of the sample weight is lost. The low temperatures of methanol loss indicate that this is lattice held. The water release in different steps suggests different ways of binding (lattice and coordinated water). Repeated thermograms for complex **5** showed low residues (~10%) and varying final decomposition patterns, indicating partial sublimation.

The three complexes are diamagnetic as expected.

TABLE II gives diagnostic i.r. and far-i.r. bands. In the ν (OH) region, the spectra of the complexes show three broad bands. The broad character of the bands indicates the existence of intense hydrogen bonding. The band between 3500 and 3430 cm^{-1} is attributed to water and methanol. The presence of coordinated hydroxides is manifested by a medium band between 3560 and 3520 cm^{-1}. The spectra also exhibit a weaker band at lower frequencies;this is apparently due to the presence of a non-deprotonated phenolic OH group in the complexes. In the spectra of all the three complexes only one band is attributed to $\nu_{as}(CO_2^-)$ and to $\nu_s(CO_2^-)$, in agreement with the existence of one type of carboxylato coordination [9]. For the three Zn(II) complexes $\Delta_{complex} > \Delta_{\text{sodium salt of the ligand}}$ ($\Delta = \nu_{as}(CO_2^-) - \nu_s(CO_2^-)$); this suggests that the carboxylate group of $hydcafH^{2-}$, $cafH^{2-}$ and fer^{2-} is coordinated as a monodentate ligand [9]. All complexes exhibit strong ν(Zn-O) bands in the far-i.r. region. Zn-O stretches are never strong bands in the i.r. spectra. The intense bands observed in the far-i.r. spectra of **4** , **5** and **6** might indicate overlap of bands due to ν(Zn-O) with bands due to other (possibly deformation) vibrational modes.

Titration curves for deprotonation and coordination reactions in a MeOH:H_2O 9:1 solution are shown in FIG.1. In the titrations , which were conducted in the presence of metal cation , the metal:ligand ratio was 1:2.

TABLE II. Characteristic i.r. bands (cm^{-1})

Assignment	$hydcafH_3$ 1	$hydcafH_2Na.H_2O$	$cafH_3$ 2	$cafH_2Na.H_2O$	$ferH_2$ 3	$ferHNa.H_2O$	4	5	6
$\nu(OH^-)_{OH^-}$							3520mb	3560m	3560m
$\nu(OH)_{MeOH,H2O}$		3600s		3600s		3600s	3430sb	3500sb	3460sb
$\nu(OH)_{phenolic}$	3420m	3410m	3421m	3420m	3440m	3435m	3400m	3340m	n.o.
$\nu(OH)_{acid}$	3386,2943s		3243,2850		2920,2860m				
$\nu(C=O)_{acid}$	1686s		1663s		1690s				
$\nu_{as}(CO_2^-)$		1480s		1468s		1472s	1570s	1490s	1500s
$\nu_s(CO_2^-)$		1320s		1346s		1347s	1270m	1275m	1265s
ν(Zn-O)							500sb	520s,405m	570s,470m

n.o.(not observed).

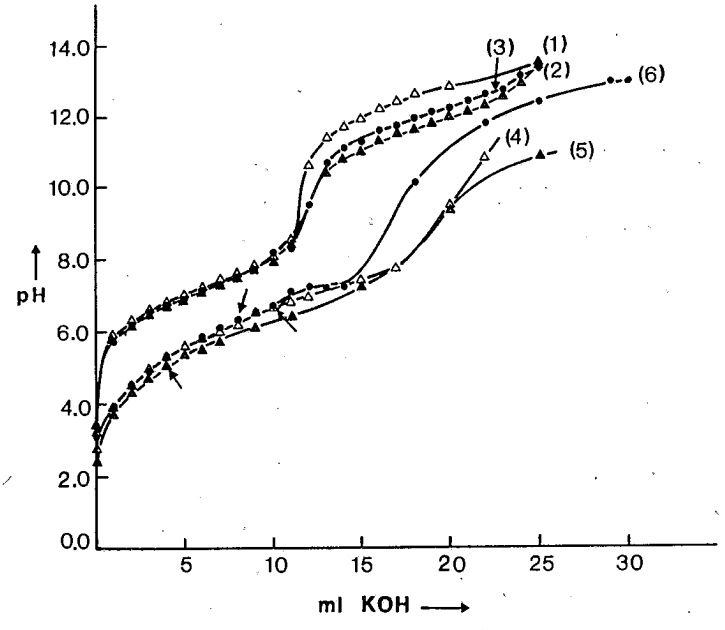

FIG.1.: *Titration curves of solutions of hydrocaffeic, caffeic and ferulic acids (1,2,3) and their mixtures with zinc(II) (4,5,6).*

1,4 : hydcafH$_3$, hydcafH$_3$/ZnCl$_2$

2,5 : cafH$_3$, cafH$_3$/ZnCl$_2$

3,6 : ferH$_2$, ferH$_2$/ZnCl$_2$

↓ *: complex precipitation*

Precipitation of the complexes occurs at relatively low pH values (6.6, 5.1 and 6.3) for **4**,**5** and **6**, respectively, before all of the carboxylic and phenolic protons of the ligands are ionised. The ligands are mostly present in the form of dianions. The pK_1 values are approximately 7.0 for the three ligands.

TABLE III gives the ^1H n.m.r. chemical shifts for $cafH_3$, **5**, $ferH_2$ and **6** in d_6-DMSO.The solubility of **4** was too low to obtain spectra of sufficient quality. The non-appearance of the carboxylic proton in the spectra of both complexes, the occurence of only one-OH signal in **5** and the absence of this signal from the spectrum of **6** confirm that caffeic and ferulic acids are coordinated to Zn(II) in their dianionic forms. As compared to the spectra of the free ligands the signals of the CH protons (both aromatic and non-aromatic) in the spectra of the complexes are slightly shifted to higher fields. These changes are due to several opposite effects, like the electric field caused by complexation, temperature independent paramagnetism of zinc (II) etc.

From the presented data, i.e. the i.r. bands and the potentiometric and thermogravimetric features , it is concluded that the dianions of the three ligands exhibit a real ambidentate character , i.e. in addition to the chelation *via* the catecholate sites, the carboxylate can also simultaneously coordinate to the zinc(II) ions, leading to the formation of oligomeric species with ligand to zinc molar ratios of 1:1, regardless of the ligand to metal ratio in the reaction mixtures. The proposed structures of the complex ions are shown in FIG.2.

In aqueous solution the mononuclear bis-(caffeate) complex of zinc(II) appears as a relatively minor species, the mononuclear tris-(caffeate) complex being the major zinc(II) compound. The predominant complexation mode in the bis and tris complexes is metal chelation at the catecholate site, resulting in coordination numbers ranging from 4 to 6 [10].

TABLE III. ^{1}H n.m.r. chemical shifts (ppm) [a,b,c,d] for $cafH_3$, $ferH_2$, **5** and **6** in d_6-DMSO.

Compound	$-CO_2H$	-OH	Aromatic protons	Non-aromatic CH	$-CH_3$
$cafH_3$	12.10sb	9.55sb,9.15sb	7.40d,7.05d,6.95mt	6.75d,6.15d	
5		8.30s	7.19d,6.94s,6.83d	6.70d,6.12d	
$ferH_2$	12.00sb	9.55sb	7.47d,7.25d,7.05mt	6.78d,6.35d	3.80s
6			7.28d,7.15s,6.96d	6.75d,6.32d	3.80s

[a] Spectra recorded at ambient temperature. [b] Me_4Si internal standard. [c] The spectra were run 10 min. after dissolution. [d] The integration of the signals is consistent with the assignments b:broad; d:doublet; mt:multiplet; t:triplet.

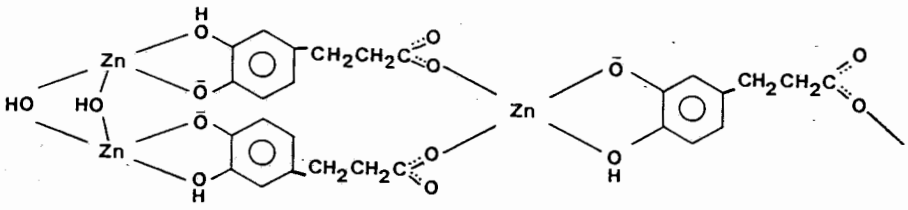

$$\left[Zn_3 (hydcaf H)_3 (OH)_2 \right]^{2-}$$

(4)

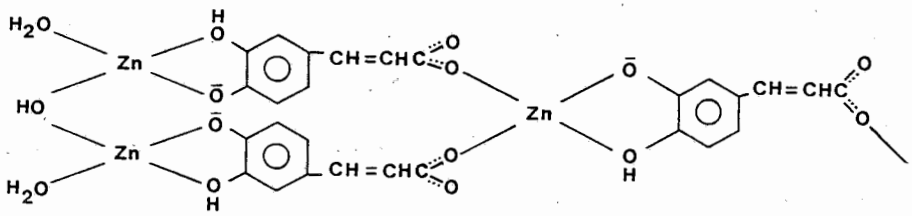

$$\left[Zn_3 (caf H)_3 (OH) (H_2O)_2 \right]^{-}$$

(5)

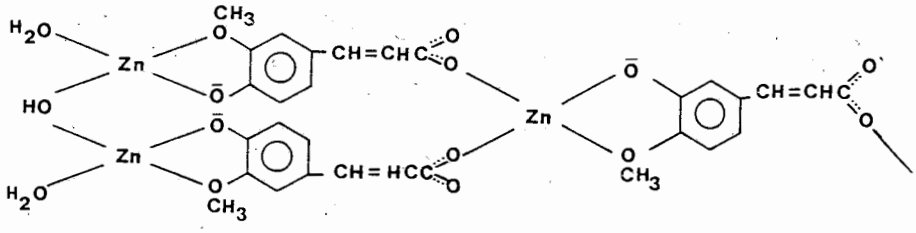

$$\left[Zn_3 (fer)_3 (OH)(H_2O)_2 \right]^{-}$$

FIG.2.: *The proposed structures of the prepared complexes in the solid state.*

The differences in the nature of the complexes formed in our systems (in 90% methanol) can be ascribed to the greater basicity of the mixed solvent[10]. The more favorable change in entropy through neutralization with potassium hydroxide in 90% methanol could be one reason for the difference and might be considered as a manifestation of the so-called "basicity" effect [11] on changing from water to water-methanol mixtures.

In the case of copper (II), nickel(II) and iron (III) with the same ligands, regardless of the ratio of ligand to metal present in the preparation mixtures, tetrahedral 1:1 complexes are prepared where the metal ions are bonded with the ligands by O^-, OH or Cl^- bridges. A 1:2 (metal : ligand) complex can be formed only for cobalt(II) with the dianion of hydrocaffeic [5] and ferulic acid [12] . Binuclear vanadium(V) and vanadium(IV,V) complexes have been prepared with the same ligands [13] with square pyramidal structures and catecholic - type of coordination with ligand to vanadium molar ratios of 3:2, 1:2 and 2:2 for hydrocaffeic, caffeic and ferulic acids , respectively , regardless of the ligand to metal ratio in the reaction mixtures.

X-ray structural investigation of the prepared compounds is at present lacking due to difficulties in obtaining convenient monocrystals.

ΠΕΡΙΛΗΨΗ

Ολιγοπυρηνικά σύμπλοκα ψευδαργύρου (II) των διανιόντων των υδροκαφεϊκού, καφεϊκού και φερουλικού οξέων

Παρασκευάσθηκαν και μελετήθηκαν ολιγομερή σύμπλοκα του ψευδαργύρου (II) με τα οξέα υδροκαφεϊκό, καφεϊκό και φερουλικό, σε διαλύματα με αναλογία μεθανόλη : νερό 9 : 1. Στα σύμπλοκα δόθηκαν οι εμπειρικοί τύποι $K_2[Zn_3(hydcafH)_3(OH)_2].2H_2O.MeOH$, $K[Zn_3(cafH)_3(OH)(H_2O)_2].H_2O.2MeOH$, $K[Zn_3(fer)_3(OH)(H_2O)_2].H_2O.MeOH$. Η ταυτόχρονη σύμπλεξη του ιόντος Zn(II) και στην καρβοξυλική και στις κατεχολικές θέσεις, η

οποία οδηγεί στον σχηματισμό τετραεδρικών ολιγομερών σωματιδίων με γραμμομοριακό λόγο υποκαταστάτη πρός ψευδάργυρο 1 : 1, υποστηρίζεται από φασματοσκοπικά (υπερύθρου, άπω-υπερύθρου, πυρηνικού μαγνητικού συντονισμού) , θερμοσταθμικά και ποτενσιομετρικά δεδομένα, στοιχειακές αναλύσεις και μετρήσεις αγωγιμότητας.

ACKNOWLEDGEMENTS

We wish to thank the Universities of Athens and Patras for financial support of the work. We thank referees for a series of helpful comments.

REFERENCES

1. Sigel H., *Metal ions in biological systems* , **6** , chapter 1 , (1976).
2.Lindsay,W.L., *In the plant root and its environment,* Ed. E.W.Carson, p.507, University Press of Virginia, Charlottesville, (1974).
3. Linder P.W. and Voye A., *Polyhedron*, **6**, 53 (1987) and references therein.
4. Peppercorn M.A. and Goldman,P., *J.Bacteriol.*, **108**,996 (1971).
5. Petrou A.L., Koromantzou M.V. and Tsangaris J.M., *Transition Met. Chem.*, **16**, 48 (1991).
6. Schwarzenbach G.and Flaschka H. (transl. revis. by H.M.N.H.Irving), *Complexometric Titrations,* 2nd edit. Methnan Co. Ltd. London (1957), A.I.Vogel, *A Textbook for Quant. Inorg. Analysis,* Longmans Co. (1961).
7.(a)Kabanos T.A. and Tsangaris J.M., *J.Coord. Chem.*, **13**, 89 (1984).
(b) Rahman A.A., Nicholls and Tsangaris J.M., *J.Coord. Chem.*, **14**, 327 (1986).
(c)Hondrellis V., Perlepes S.P., Kabanos T.A. and Tsangaris J.M., *Synth. React. Inorg. Met.-Org. Chem.*, 83 (1988).
8.Geary W.J., *Coord. Chem. Rev.*, 7, 81 (1971).
9.Deacon G.B. and Phillips R.J., *Coord. Chem. Rev.*, **33**, 227 (1980)
10.Tvson C.A. and Martell A.E.,*J.Amer. Chem. Soc.*, **90**, 3379 (1968).
11.Franks F. and Ives D.J.G., *Quart. Rev.,* (London), **20**, 40 (1966).
12. Petrou A.L., Koromantzou M.V. and Tsangaris J.M.,*Chimika Chronika, New Series* ,**22**, 189, (1993).
13.Petrou A.L. *Transition Met. Chem.*, **18**, 462 (1993).

Abbreviations

Hydrocaffeic acid	abbr. hydcafH_3
Caffeic acid	abbr. cafH_3
Ferulic acid	abbr. ferH_2

Chimika Chronika, New Series, 24, 147-158 (1995)

COMPARISON OF THREE PROCEDURES FOR RUBISCO PURIFICATION FROM GREEN TOBACCO LEAVES

E. HASSIOTOU AND A. TSAFTARIS
Department of Genetics and Plant Breeding
Aristotelian University of Thessaloniki
54006 Thessaloniki, Greece

Received: January 21, 1994

Ackowledgement

The authors are thankful to Dr. N. Ioannides and Dr. P. Lolas of Tobacco Institute of Drama, Greece, for providing the tobacco seeds.

SUMMARY

Highly purified Rubisco has been extracted from tobacco leaves (Greek varieties TA21, ΚΠ-S_2) by crystallization. Of the three different procedures applied, two resulted in a partial purification of the enzyme: the third one gave crystalline Rubisco. Identification of the crystalline material with Rubisco was made by gel electrophoresis. The isolation of pure form of this protein was a prerequisite for the development of an immunological quantitative determination of Rubisco, in order to study Rubisco variability in different tobacco varieties and different developmental stages.

Key words: Rubisco, purification, crystallization, tobacco

Abbreviations

Rubisco: Ribulose 1,5 bisphosphate carboxylase/oxygenase
LS: Large Subunit of Rubisco
SS: Small Subunit of Rubisco
TCA: Trichloroacetic acid
SDS-PAGE: Sodium Dodecyl Sulphate Polyacrylamide Gel Electrophoresis

INTRODUCTION

Recently, as the needs for new sources of high quality protein has become crucial, nonconventional sources have been tapped for the production of proteins which meet nutritional standards and requirements for human and animal consumption. The most abundant protein in higher plant chloroplasts is Rubisco, the bifunctional enzyme that catalyzes the initial reactions of photosynthetic and respiratory pathways (Kawashima and Wildman 1970, Chan and Wildman 1972, Gray et al 1976, Jensen and Bahr 1977, Johal and Bourque 1979, Miziorko and Lorimer 1983). Rubisco from higher plants and eucaryotic algae is a hexadecamer composed of eight 50-60 KDa, chloroplast encoded "large" subunits, and eight 12-20 KDa, nuclear encoded "small" subunits (Kawashima et al 1971, Chan and Wildman 1972, Gray et al 1976, Chen et al 1976, Johal and Bourque 1979, Müller et al 1983).

On the basis of comparative studies, Staron (1980) concluded that tobacco leaves were a preferable source of high quality leaf protein and it was proposed to exploit the commercial possibility of using tobacco Rubisco for human food and medicine (Ershoff et al 1978, Tso and Kung 1979, Fantozzi 1985). With an exception of a slightly lower level of methionine, its amino acids profile equals or exceeds that of the F.A.O. pattern (Tso and Kung 1979, Fantozzi 1985). Besides, Rubisco has a high content of lysine, threonine and valine, contrary to other abundant plant proteins, like seed proteins (Tso and Kung 1979).

Reliable methods for Rubisco quantitative determination are a necessary prerequisite to study the extraction efficiency for pure Rubisco protein, the variation of its level among different tobacco varieties and different developmental stages, the influences of various cultivating practices upon its content e.t.c. Methods based upon the activity of the enzyme proved to be inaccurate, since it does not reflect the total amount of the protein but only its enzymatically active form. This paper describes three procedures for Rubisco purification from Greek tobacco cultivars in crystalline form, in order to obtain the anti-Rubisco antibodies necessary for the development of an immunological determination of total Rubisco (Hassiotou and Tsaftaris 1988, Hassiotou and Tsaftaris 1991).

MATERIALS AND METHODS

Plant material

Nicotiana tabacum, KII- S_2, TA/ 21 (local varieties of oriental type) grown by conventional agronomic practices at normal density population (spacing 20 cm x 50 cm). Seeds were provided by the Greek Tobacco Institute.

Rubisco purification

Various procedures developed in the past for Rubisco purification from different plant species like spinach, alfalfa and tobacco were applied either identical or in combination for Rubisco purification from oriental type Greek tobacco cultivars.

Methods of Johal and Bourque (1979)

Reagents:

Buffer A: 25 mM Tris-HCl, pH 8
1mM EDTA
1.0 mM b-mercaptoethanol

$(NH_4)_2SO_4$ (37 and 50 percent saturation)

65 g of tobacco leaves were homogenized in 50 ml of buffer A, filtered and centrifuged (7,000 g, 45 minutes). A 37 % to 50 % saturated $(NH_4)_2SO_4$ precipitate was prepared; after recovery of the precipitate by centrifugation it was redissolved in 20 ml of buffer A and passed through a Sepharose 4B column. Twenty fractions containing protein were collected and the optical density at 280 nm was measured (Fig. 1). The fractions 6 - 13, that showed the highest optical density, were pooled and subjected to further purification through a DEAE-cellulose column. The optical density at 280 nm of the first 60 fracions was measured (Fig. 2).

Method of Kung et al (1980)

Reagents

Buffer A: 25 mM tris-HCl
0.2 mM EDTA, pH 7.4
10 % Na_2EDTA
5% TCA

100 g of tobacco leaves were homogenized in 32.5 ml NaCl and 0.175 ml b-mercaptoethanol, filtered and heated to 15- 20 °C and the pH was adjusted to 7.4. The suspension was centrifuged (10 minutes, 35,000 g) and the sumernatant was passed through a Shephadex G- 50 column, equilibrated with buffer A. Fractions containing protein were collected and crystals usually were formed overnight at 4 °C.

Modified method of Chan et al (1972)

Reagents

Buffer A: 0.5 M Tris - HCl, pH 7.4
1.0 M NaCl
0.001 M EDTA
0.002 M $MgCl_2$
0.08 M b-mercaptoethanol

Buffer B: 0.025 M Tris - HCl, pH 7.4
0.20 M NaCl
0.0005 M EDTA

Buffer C: 0.025 M Tris - HCl pH 7.4
0.0005 M EDTA

5 % TCA

15 g of tobacco leaves were homogenized in 15 ml of ice-cold buffer A in an ice bath, filtered and centrifuged (17,000 g, 5 minutes). The supernatant was centrifuged again (17,000 g, 30 minutes). The new supernatant was passed through a G - 50 Sephadex column (1 by 50 cm) previously equilibrated with buffer B. The first 12 ml of eluate containing protein were collected and concentrated to 3 ml and centrifuged (2,500 g, 5 minutes). After the addition of $NaHCO_3$ (0.002M) and $MgCl_2$

(0.003M) the material was incubated for 30 minutes at room temperature and was dialyzed against buffer C. Rubisco crystals appeared overnight. Crystals were dissolved with buffer B and the material was dialyzed against buffer C as before. Crystals appeared in a few hours.

SDS - Electrophoresis

SDS - Polyacrylamide Electrophoresis was performed according to the method of Laemmli to evaluate the purity of the enzyme. The separating gel contained 12 % while the stacking gel 5 % acrylamide. Gels were run at 30 mA for 6-7 hours and were stained with Coomassie Brilliant Blue. Sigma pure Rubisco from spinach was co-electrophoresed in the polyacrylamide gels as a marker.

RESULTS AND DISCUSSION

Three different procedures were used for the purification and crystallization of Rubisco from tobacco leaves of the orientl type Greek varieties KΠ-S_2 and TA/21, two months after transplanting in the field.

The method of Johal and Bourque (1979) and the method of Kung et al (1980) were not satisfactory since they ended in a partial purification of the enzyme, while the modified method of Chan et al (1972) yielded crystalline Rubisco.

Especially the use of the method of Johal and Bourque failed to form crystals. Figure 1 shows the optical density of the first 20 fractions collected from the Sepharose 4B column. Fractions 6-13 that showed the highest optical density were pooled and subjected to further puriffication.

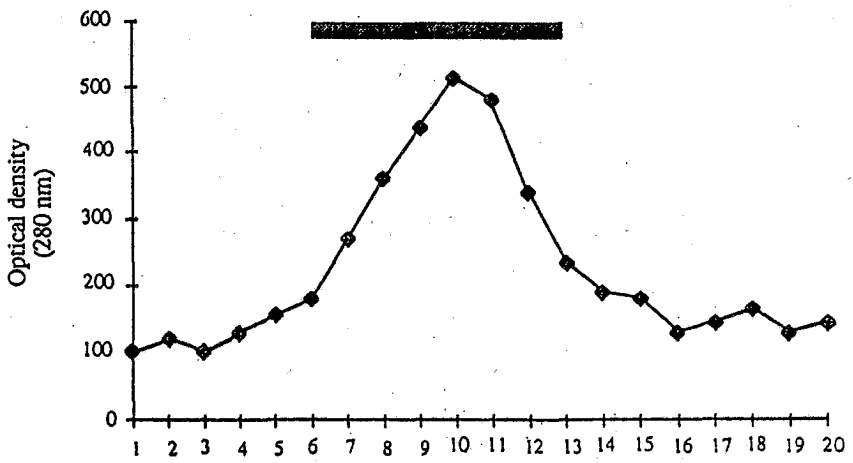

Fig. 1. Absorbance profile of the first 20 fractions eluted from a Sepfarose-4B column.

The optical density of 20 fractions from the DEAE-cellulose column is illustrated in Figure 2. Fractions 52 and 54 showed the highest optical density.

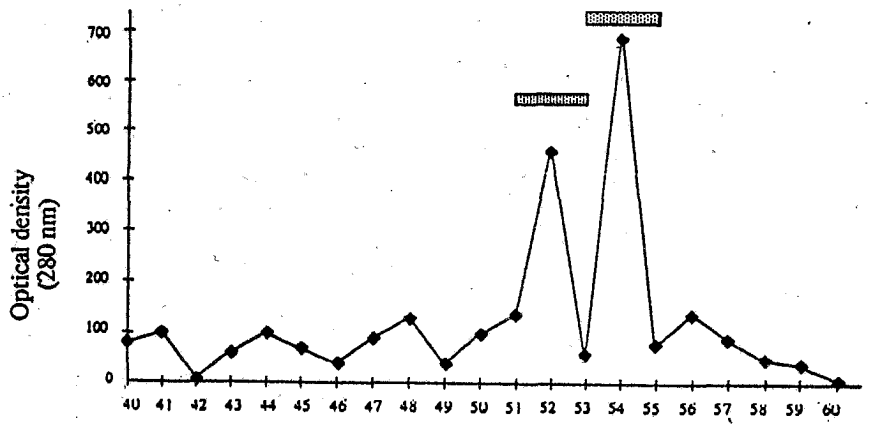

Fig 2. Absorbance profile (280 nm) of 20 fractions eluted from a DEAE- cellulose column.

The SDS - PAGE profiles of these two fractions indicate that Rubisco purity was not satisfactory (Fig. 3), since they were resolved in more than the two typical bands of Rubisco. The moderate efficiency of this method led to the use of the posterior method of Kung et al (1980).

According to Chan et al (1972) tobacco Rubisco is soluble only in the presence of Ribulose bisphosphate (RuBP) or high salt (NaCl). Heat treatment is also required for maximum activity of the enzyme (Kung et al 1980). The recent simplification of the crystallization procedure is based upon these properties of Rubisco. The addition of $NaHCO_3$ and $MgCl_2$ was not necessary for crystallization, although their presence is decisive for crystal formation in other methods methods (Chan et al 1972). This method resulted in Rubisco crystallization; but the appearance of additional bands in SDS - PAGE electrophoresis indicates that the final product is not homogenous (Fig. 4). This contrasts with the result of Johal and Bourque (1979) and Kung et al (1980) who assert the production of crystalline Rubisco. Crystallization, in general, is a complex phenomenon and the molecular forces which cause proteins to crystallize are poorly understood. The nature and concebtration of electrolytes present in the medium, the pH and concentration of the protein are crucial factors which influence the crystallization process. Besides, the fact that these two methods were inefficcient with our plant material perhaps is due to differences in the chemical composition of leaves. Especially the extractability, protein quality and protein yield is significantly influenced by the concentration of polyphenols and other secondary metabolites. Polyphenol - protein binding occurs immediately under certain conditions, reducing the extractability, protein quality and protein yield (De Jong 1984). Polyphenol determination was carried out in 15 tobacco varieties and indeed TA21 and KH-S_2 showed low polyphenol content (Hassiotou and Tsaftaris1991). For this determination we used Folin - Denis method, because it is nonspecific for any group of polyphenols (simple phenolics, non-tannin flavans, hydrolysable tannins and condensed tannins) ((Peri and Pompei 1971, Burns 1963).

Subsequently a third purification procedure was applied, the modified method

of Chan et al (1972). This method is based on the property of Rubisco to be extremely insoluble in the absence of ribulose-1,5-diphosphate and in the presence of Mg^{2+} and HCO_3^-.

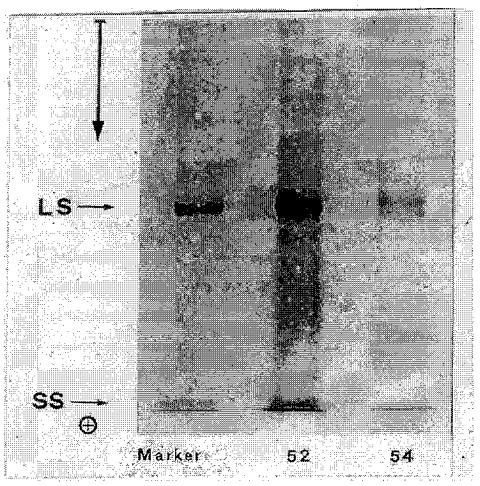

Fig. 3. SDS-PAGE (12 % polyacrylamide) of two fractions (52, 54) of the final product prepared by the method of Johal and Bourque. Crystalline spinach Rubisco was used as a marker.

The homogenization step is necessary to be carried out at 0 °C, otherwise may result in enzyme degradation. According to results of Paech and Dybing (1986) proteolytic degradation of Rubisco caused complete loss of catalytic activity, because of prolonged purification procedures.

In our attempt to remove the low molecular weight substances we used gel filtration chromatography. The Sephadex G- 50 (coarse) column was more efficient than G - 25 proposed by Chan et al (1972). Another modification concerned the degree of the eluate concentration. Reduction to 1/4 of the initial volume, instead of the proposed to 1/3, assured an easier crystallization. Also there was no addition of NaCl after the eluate concentration and before the incubation. Another modification refers to eluate incubation, which took place at room temperature for 30 minutes, instead of the incubation proposed at 30 °C for 15 minutes.

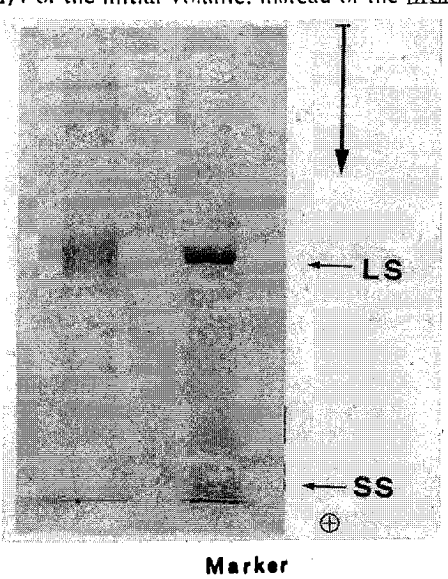

Fig. 4. SDS-PAGE (12 % polyacrylamide) of tobacco Rubisco purified by the method of Kung et al. Spinach crystalline Rubisco was used as a marker.

Crystallization was achieved by this method. Crystal formation was highly dependent on the proper combination of protein concentration, pH, and NaCl concentration. The relation between protein concebtration and NaCl concentration seems to be the most critical factors.

A recrystallization of crystalline Rubisco was carried

out. Crystal formation accelerated at ice-box temperature during the first and second crystallization procedure. Crystals appeared in a few hours, maximum yield was obtained after 15 hours. The recovery of protein achieved after each recrystallization was only 30 - 40 %.

Analysis of the final recrystallized Rubisco by SDS-electrophoresis revealed two polypeptides, corresponding to the large and small subunits of Rubisco, indicating that the protein is highly pure (Fig. 5). Crystalline enzyme preparations stored for 2 - 3 months at -22 °C resulted inb its degradation; SDS - PAGE did not show the two typical bands of the purified enzyme but more bands (Fig. 6).

Comparisons of Rubisco purified from the two cultivars revealed no differences in size behaviour on SDS gels and in homogeneity in the three procedures.

Recently, Rubisco purified by this last method was used as antigen source for antibody production in rabbits with very good results. Subsequemtly these antibodies were used for the development of a reliable method of quantity determination of Rubisco protein in tobacco crude leaf extract in order to estimate the variation of Rubisco protein content in Greek tobaco cultivars and the optimum time of harvest for the maximization of its extraction (Hassiotou and Tsaftaris 1991). KH-S_2

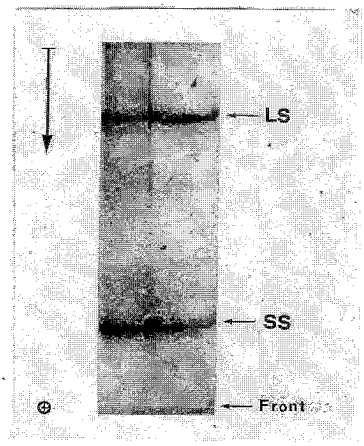

Fig. 5. SDS-PAGE (12 % polyacrylamide) of tobacco Rubisco purified by the method of Chan et al.
LS: large subunit
SS: small subunit

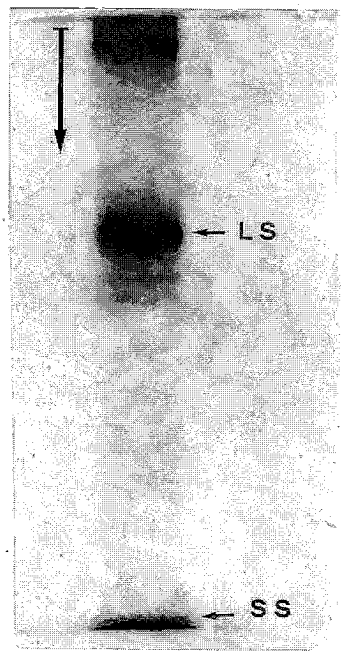

Fig. 6. SDS-PAGE (12 % polyacrylamide) of crystalline Rubisco, after a two-month storage at - 22 °C.

and TA21 were found to be promising in respect to high Rubisco and low polyphenol concentration. Papakosta et al (1985) using similar tobacco varieties found a higher Rubisco content; this was expected because, apart from the different varieties it was applied a different determination method (based on the measurement of the OD_{590} of Rubisco band on a polyacrylamide gel) and different developmental stages and population densities.

ΣΥΓΚΡΙΣΗ ΤΡΙΩΝ ΜΕΘΟΔΩΝ ΠΑΡΑΛΑΒΗΣ ΚΑΘΑΡΟΥ RUBISCO ΑΠΟ ΠΡΑΣΙΝΑ ΦΥΛΛΑ ΚΑΠΝΟΥ

ΠΕΡΙΛΗΨΗ

Υψηλής καθαρότητας Rubisco εκχυλίσθηκε από φύλλα καπνού (ελληνικές ποικιλίες TA21, ΚΠ-S_2) με τη μέθοδο της κρυστάλλωσης. Από τις τρεις διαφορετικές μεθόδους που εφαρμόστηκαν, οι δύο έδωσαν μερικώς καθαρό ένζυμο, ενώ η τρίτη έδωσε Rubisco σε κρυσταλλική μορφή. Η ταυτοποίηση του προκύψαντος κρυσταλλικού υλικού ως Rubisco έγινε με χρήση gel ηλεκτροφόρησης. Η απομόνωση της πρωτεΐνης αυτής σε καθαρή μορφή ήταν απαραίτητη για την ανάπτυξη ανοσιολογικού ποσοτικού προσδιορισμού του Rubisco, ώστε να μελετηθεί η παραλλακτικότητά του σε διαφορετικές ποικιλίες καπνού και σε διαφορετικά στάδια φυτικής ανάπτυξης.

Ackowledgement

The authors are thankful to Dr. N. Ioannides and Dr. P. Lolas of Tobacco Institute of Drama, Greece, for providing the tobacco seeds.

REFERENCES

Chan, P.H., and Wildman, S.G. 1972. Chloroplast DNA codes for the primary structure of the large subunit of Fraction I protein. Biochim. Biophys. Acta 277: 677-680.

Chan, P.H., Sakano, K., Singh, S., and Wildman, S.G. 1972. Crystalline Fraction I protein: Preparation in large yields. Science176: 1145-1146.

Chen, K., Johal, S., and Wildman, S.G. 1976. Role of chloroplast and nuclear DNA genes during evolution of Fraction I protein.In:Bucher et al (eds): "Genetics and Biogenesis of chloroplasts and mitochondria". Holland Biomed. Press. Amsterdam. al. Edit. Elsevier/N. Holland. Amsterdam: 3-11.

De Jong, D.W.1984. Factors related to maximization of protein extraction from green leaves of tobacco, Nicotiana tabacum L..In.:Singh (ed): "Current trends in Life sciences XI". Tod. & Tom.'s Print. Public., N.Delhi: 9-20.

Ershoff, B.H., Wildman, S.G., and Kwanyuen, P.1978. Biological evaluation of crystalline fraction-I-protein from tobacco. Proc. Soc. Exp. Biol. Med. 157: 626-630.

Fantozzi, P. 1985. Tobacco as protein source: protein extraction and purification technology. Proc. of a round table held at Salsomaggiore: 29-49.

Gray, J.C., Kung, S.D., and Wildman, S.G. 1976. Polypeptide chains of the large and small subunit of Fraction I protein. In:Bucher et al (eds): "Genetics and Biogenesis of chloroplasts and mitochondria". Holland Biomed. Press, Amsterdam.

Hassiotou E. and A.S. Tsaftaris. 1990. Immunological determination of the enzyme ribulose 1,5 bisphosphate carboxylase/oxygenase in tobacco. Corresta Symposium Halkidiki.

Hassiotou E. and A.S. Tsaftaris. 1991. Genetic variability for Rubisco protein and polyphenol content in fifteen tobacco (N. tabacum) cultivars. J. Agronomy and Crop Science 167: 103-111.

Jensen, R.G., and Bahr, J. T. 1977. Ribulose 1.5-bisphosphate carboxylase/ oxygenase. Ann. Rev. Plant Physiol. 28: 379-400.

Johal, S., and Bourque, D.P. 1979. Crystalline ribulose 1,5-bisphosphate carboxylase/oxygenase from spinach. Science 204: 75-77.

Kawashima, N., and Wildman, S,G. 1970. Studies on Fraction-I protein.I.Effect of crystallization of Fraction-I protein from tobacco leaves on ribulose diphosphate carboxylase activity. Biochim. Biophys. Acta 229: 240-249.

Kawashima, N., and Wildman, S.G. 1972. Studies of Fraction I protein. IV.Mode of inheritance of primary structure in relation to whether chloroplast or nuclear DNA contains the code for a chloroplast protein. Biochim. Biophys. Acta 262: 42-49.

Kawashima, N., Kwok, S./Y., and Wildman, S.G. 1971. Studies on Fraction 1 protein. III.Comparison of the primary structure of the large and small subunits obtained from five species of Nicotiana. Biochim. Biophys. Acta 236: 578-586.

Kung, S.D., Chollet, R., and Matsho, T.V. 1980. Crystallization and assay procedures of tobacco ribulose-1,5-bisphosphate carboxylase/oxygenase. Methods in enzym. 69: 326-336.

Miziorko, H.M., and Lorimer, G.H. 1983. Ribulose-1,5-bisphosphate carboxylase/oxygenase. Ann.Rev. Bioch. 52: 507-535.

Müller, K./D., Salnikow,J., and Vater,J. 1983. Amino-acid sequence of the small subunit of D-ribulose-bisphosphate carboxylase/oxygenase from Nicotiana tabacum. Biochim. Biophys. Acta 742: 78-83.Staron, T. 1980. Le Tabac. Bulletin du Station des Antibiotiques et des Bioconversions: 353.

Paech, C., and Dybing, C.D. 1986. Purification and de-gradation of ribulose bisphosphate carboxylase from soybean leaves. Plant Physiol. 81: 97-102.

Papakosta D., Gagianas A. A., and Sfikas A.G. 1985. Fraction I leaf protein content ang yield of Greek tobacco cusltivars at two plant population densities. J. Agronomy and Crop Science 154: 250-257.

Pirie,N.W. 1987. Human trials and experiments. In: Leaf protein and its by-products in human and animal nutrition. Cambridge Univers. Press: 105-123.

Tso, T.C., and Kung, S.D. 1979. In: Telek Graham (ed): "Leaf protein concentrates".AVI Publ. Comp., Connecticut.

Chimika Chronika, New Series, 24, 157-171 (1995)

A STUDY OF THE ELECTROCHEMICAL REDUCTION OF U^{VI} ON U AND EBONEX

Y. TYROVOLAS

Dpt. of Chemical and Process Engineering, University of Newcastle upon Tyne, *Newcastle upon Type*, NE1 7RU, England, U.K.

(Received April 18, 1994)

ABSTRACT

The electrochemical reduction of U^{VI} has been studied on U and Ebonex cathodes. Polarisation and current efficiency curves were obtained for each cathode material describing the performance of the electrolytic reduction of U^{VI} on each cathode. The performance of these two cathode materials under study was compared with the one of Ti for the above reaction. A limited investigation of the electrochemistry of U was carried out, and the existence of two states of U metal in uranyl nitrate/nitric acid solutions were confirmed.

Key words : Electrolytic reduction of U^{VI}, Electrochemical behaviour of U, Electrochemical behaviour of Ebonex.

INTRODUCTION

The electrolytic reduction of U^{VI} is used [1,2] for the separation of Pu from U in the Purex process [3, 4, 5, 6] a method used for the reprocessing of spent nuclear fuels. The feasibility of the method has been demonstrated by pilot plant experiments [7, 8, 9] indicating Ti to be the preferred cathode material. Due to Ti dissolution during the electrolytic process Ti ions are introduced into the system creating additional waste disposal problems. A step forward is to replace Ti with U, which doesn't introduce foreign ions into the solution. An alternative proposal is the use of Ebonex as cathode instead of Ti. Ebonex is a recently invented ceramic material based on Ti oxides extremely resistant to corrosion. Both Uranium and Ebonex have never been used before as cathodes and the information in the literature concerning their electrochemical behaviour is extremely limited.

The scope of the present work is to investigate the electrolytic reduction of U^{VI} on U and Ebonex and to compare the performance of the new cathode materials with that of Ti. At the cathode there are three groups of electrochemical reactions taking place. The hydrogen evolution reaction, the reduction of nitric acid and the electrolytic reduction of U^{VI} (10, 13) shown by the equation below:

$$UO_2^{2+} + 4H^+ + 2e \rightarrow U^{4+} + 2H_2O$$

These reactions have been discussed briefly elsewhere (11, 12). Hydrazine is expected to be stable. At the anode, the oxygen evolution and the oxidation of hydrazine take place.

Ti is a well-known metal exhibiting active-passive behaviour (14), the presence of a hydride film has also been reported (15). The electrolytic reduction of U^{VI} on Ti has been studied extensively [11, 12, 13]. The presence of uranyl nitrate has been found (12) responsible for the formation of an oxide film on the Ti surface according to a mechanism proposed by Stern (16). The performance of the electrolytic reduction of U^{VI} is significantly affected by the nature of the film covering the Ti surface (12, 13). The oxide surface seems to favour the electrolytic reduction of U^{VI} (12, 13). Equations describing the performance of the electrolytic reduction of U^{VI} on the different states of Ti have been proposed (12).

Uranium has been found exhibiting active-passive behaviour similar to Ti (17-25). In H_2SO_4 media the active state (18, 20) is in the region -0.5 to -1.0 V (S.C.E.), the transpassive starts at 0.1V (S.C.E.) and the region in between is attributed to the passive state. Nitric acid seems to have a passivating effect on U; the presence of the active state was not possible to be detected (18, 19). It is generally believed (17-25) that in acidic media U is covered by a metal oxide film, UO_2. The presence of UO_3 has been proposed by certain research workers (21, 22, 25), while the presence of UH_3 even in small quantities can not be excluded (21, 23). The reduction of certain oxidising agents such as NO_2^-, NO_3^-, CrO_4^{2-}, MoO_4^{2-}, WO_4^{2-}, at the electrode surface can cause passivation to the metal (20) according to a mechanism proposed by Stern (16) for metals exhibiting active/passive behaviour. In acidic solutions (18, 19, 22) the dissolution product of U is UO_2^{2+}. The active state of the metal is believed (20) to be covered by a protective film not allowing measurable quantities of U to enter the solution.

The investigation of the electrochemical behaviour of U metal is not so extensive as the one of Ti (14). Further investigation has to be carried out on the composition of the oxide film, the presence of the hydride film, the existence of the active/passive state and on relevant mechanisms based on quantitative results. The performance of U as a possible

cathode material on the reduction of U^{VI} has been found rather poor showing low current efficiencies and low reduction rates (29).

Ebonex is a black ceramic material extremely resistant against corrosion with an electrical conductivity similar to carbon. It is a substoichiometric oxide of Ti composed mainly form Ti_4O_7 and/or Ti_5O_9(26). It is a recently invented electrode material (27), with excellent chemical resistance and high oxygen and hydrogen overpotentials (28, 32). It doesn't form hydrides, but there is a possibility to get oxidised during an electrolytic process (28).

EXPERIMENTAL PROCEDURE

The experimental procedure followed in the present work is the same with the one used on Ti, discussed extensively elsewhere (12). Very briefly it can be summarised that the study of the electrolytic reduction of U^{VI} is based on polarisation curves and overnight preparative runs for different concentrations of U^{VI} employing a rotating disc electrode (R.D.E.) operated at 1000 r.p.m. Area of electrode U : 1.96 X 10^{-5} m^2, Ebonex : 2.80 X 10^{-5} m^2. The electrolyte used was a solution of uranyl nitrate (0.0-0.8M) in 2.0 M nitric acid/0.2 M hydrazine. The presence of hydrazine is to protect U^{IV} from NO_2^- ions (30). All potentials are corrected for the IR_{drop} using an interrupter technique (11,33) and the analysis for U^{IV} was performed on a u.v. spectrophotometer at 650 nm (11). The electrode was treated electrochemically, when necessary, in the solution to be examined on a specified current density.

RESULTS - DISCUSSION

A) *Uranium* electrode

States of Uranium

A preliminary examination of the Uranium electrode surface with an electron microscope revealed the presence of an oxide film, Fig 1 b,c. At higher cathodic potentials, -1.3 V (S.C.E.), the nature of the film changes, Fig 1d. The presence of the oxide film is generally accepted (17-25) and the passivating role of nitric acid on U has also been demonstrated (18, 20). The presence of the hydride on the U surface has not been proved in spite of the evidence for its existence (21, 23). The film covering the U surface in Fig 1d is similar to a hydride film, but in the absence of supporting reference from the literature, no such statement can be made.

Further evidence on the two states of U can be obtained by the polarisation curves in Fig 2. The electrode has been previously treated for 5 minutes at the state to be

examined i.e. at -1.4V and -0.1V (S.C.E.) respectively. The fast sweep rates (120 mV/min) show the behaviour of the reduction of U^{VI}, represented by the curves, over the examined potential region on each state of U being created by the electrode treatment at the specified potential. The different curves of U^{VI} obtained for each state indicate the dependence of the electrolytic behaviour of U^{VI} on the state of the Uranium electrode on which it takes place. Similar behaviour was obtained on a Ti electrode (12). At slower sweep rates, 2-3 mV/min, each curve has initially the characteristics of the fast sweep curve of the same U state. As the potential increases the curve of the oxide state gradually deviates from the curve of the oxide state towards the behaviour of the other state. At -1.4V (S.C.E.) the oxide curve has fully obtained the other's state character indicating a complete transformation of the surface from one state to the other. This transformation possibly takes place at approx. -0.9V (S.C.E.) demonstrated by the steep increase of the current density at that potential region. The curve of the other state, the one at -1.4V, doesn't obtain the oxide's behaviour even at very low potentials in the oxide region. This is demonstrated by the current density at -0.1V (100 A/m^2) which is 7X higher to the one of the oxide state (15 A/m^2). The location of the passive state at -0.2V to +0.1V (S.C.E.) and the active one at -0.8V to -1.1V (S.C.E.) in nitrate (20) and sulphuric acid solutions (18) is in agreement with the present work. In the absence of information concerning the active/passive states in nitric acid solutions and the existence of a hydride film, it is difficult to attribute the state at -1.1V (S.C.E.) to an active state and/or to a presence of a hydride film, although there is strong evidence towards this direction.

Polarisation curves

The polarisation curves of U^{VI} on U for different concentrations of uranyl nitrate (0.0-0.8 M) are shown in Fig 3. The overnight electrochemical treatment of the electrode at 600 A/m^2 in the solution to be examined creates a stable electrode surface on which the electrolytic reduction of U^{VI} was studied for current densities in the range of 200-1000 A/m^2. The above current density range represents the possible operating region of a spent nuclear fuel reprocessing plant. The role of current density excursions towards higher (2000 A/m^2) or lower current densities (20 A/m^2) in the above plant for time intervals up to an hour was investigated in the present work. The investigation was focused on the effect of the current density excursions on the stability of the electrode surface created by the overnight electrochemical treatment and consequently the response of the electrolyte reduction of U^{VI} on the affected electrode surface. In order to check reproducibility, the electrode was treated further for an extra day at 660 A/m^2 as before and the investigation of the electrolytic reduction of U^{VI} was repeated. The end of the electrode treatment on the oxide region for 0.0M and 0.8M U^{VI}, Fig 3 (a, d) indicates that the examination of the U^{VI} reduction will be performed on an oxide surface. Similarly the U^{VI} reduction of 0.1M and 0.3M U^{VI}, Fig 3 (b, c), will be performed on a different

surface probably a hydride one. In the presence of U^{VI} ions U seems to exhibit an active-passive behaviour according to Stern mechanism (16) which has been confirmed on U metal by Ward and Waber (20). Reasons justifying this statement is the increase of the concentration of the oxidising species (U^{VI} , NO_3^-) in the solution from 0.3M to 0.8M of uranyl nitrate. This increase causes a shift of the mixed potential from -1.1V to -0.3V (S.C.E.) in the passive region, Fig 3 (b, c, d). The only peculiarity in this case is that in the absence of U^{VI} ions, Fig 3 a, one would normally expect to find the potential of 0.0M U^{VI}, according to Stern mechanism, in the region of -1.1V (S.C.E.). In practice, the potential was found in the oxide region at -0.4V (S.C.E.) contradicting Stern mechanism. The reason for this peculiarity remains unknown.

The polarisation curves of 0.1M and 0.3M U^{VI}, Fig 3 (b, c), are practically identical. They have the same shape and lie in the same potential region. The curves when repeated on the following day were found reproducible. All these observations give evidence for the stability of the state at -1.1V (S.C.E.), which seems to be fully developed. Generally the stability of the surface was not disturbed by further treatment of the electrode at 20 A/m^2 and 2500 A/m^2, Fig 3b. The reactions seem to be sluggish for potentials up to -1.1V (S.C.E.). At higher potentials a steep increase of the current density is observed probably due to an enhancement of a competing reaction or to the presence of an additional reaction.

The curves of 0.8M U^{VI} obtained on an oxide surface, Fig 3d, were found reproducible and independent on a further treatment of the electrode at 2500 A/m^2. A treatment at 20 A/m^2 seems to have a destabilising effect of the oxide surface, shifting the curves towards negative values. This may be an indication of changes occurring on the oxide electrode surface. The oxide surface, in contrast of the other surface at -1.1V, seems to favour the electrolytic reduction of U^{VI}, as current densities up to 20x higher have been observed on this surface. At high potentials, -0.8V (S.C.E.), the current seems to approach a limiting value. Taking into account the current efficiency curves, Fig 4a, this doesn't seem to be genuine diffusion controlled limiting current plateau. This is probably due to certain changes of insulating character at the electrode surface.

The curves of the background solution (0.0M U^{VI}), Fig 3a, obtained on an oxide surface were shifted towards less negative potentials, when repeated on the following day. The second day's curves seem to have been obtained on a more stabilised electrode surface than the first day's curves, as no destabilisation effect was observed on the second day's curves by a further electrode treatment at 20 A/m^2 and 2500 A/m^2. The background current densities were found up to 1 order of magnitude higher than those of 0.3M and 0.1M U^{VI}, Fig 3 (b, c). The tendency of the curves to reach a limiting value at approx. -0.7V in a similar way to the 0.8M U^{VI} curves, Fig 3d, confirms the hypothesis of changes of insulating character occurring on the electrode surface's film.

a)

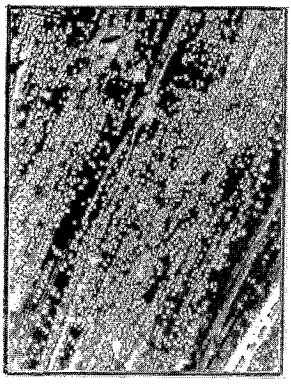

b)

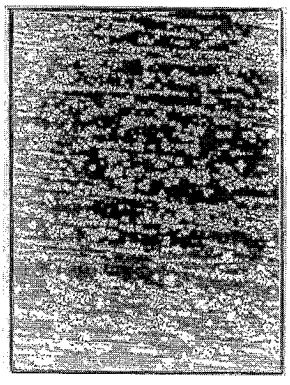

c)

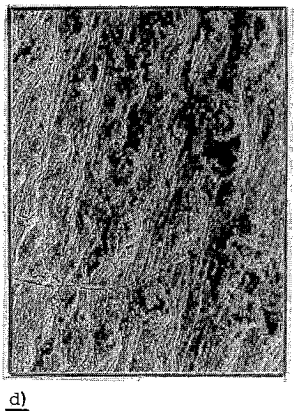

d)

Fig (1)

Photographs of the films covering the surface of a Uranium electrode taken by an electron microscope. The electrode was treated electrochemically for 5 hrs in a 2.0 M HNO_3 solution.

a) x1000 magnification. Polished electrode without electrochemical treatment.
b) x5000 magnification. Electrode treatment at -0.1 V (S.C.E.) OXIDE FILM
c) x1000 magnification. Electrode treatment at -0.5 V (S.C.E.) OXIDE FILM.
d) x1000 magnification. Electrode treatment at -1.3 V (S.C.E.) Possibly a hydride film.

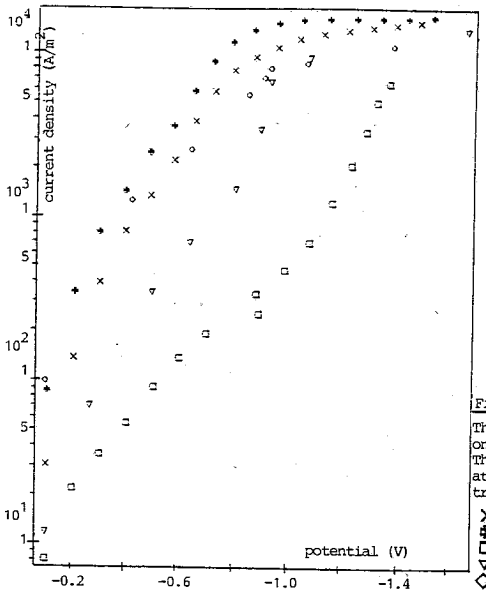

Fig (2)

The dependence of the electrolytic reduction of U^{VI} on the two different states of Uranium electrode. The polarisation curves of 0.8M U(VI) were obtained at different manual sweep rates, the electrode being treated at different potentials for 5 mins.

×: sweep rate 120 mV/min, electrode treatment at -1.4V
✱: sweep rate 40 mV/min, electrode treatment at -1.4V
□: sweep rate 120 mV/min, electrode treatment at -0.1V
▽: sweep rate 2 mV/min, electrode treatment at -0.1V
◇: sweep rate 3 mV/min, electrode treatment at -1.4V

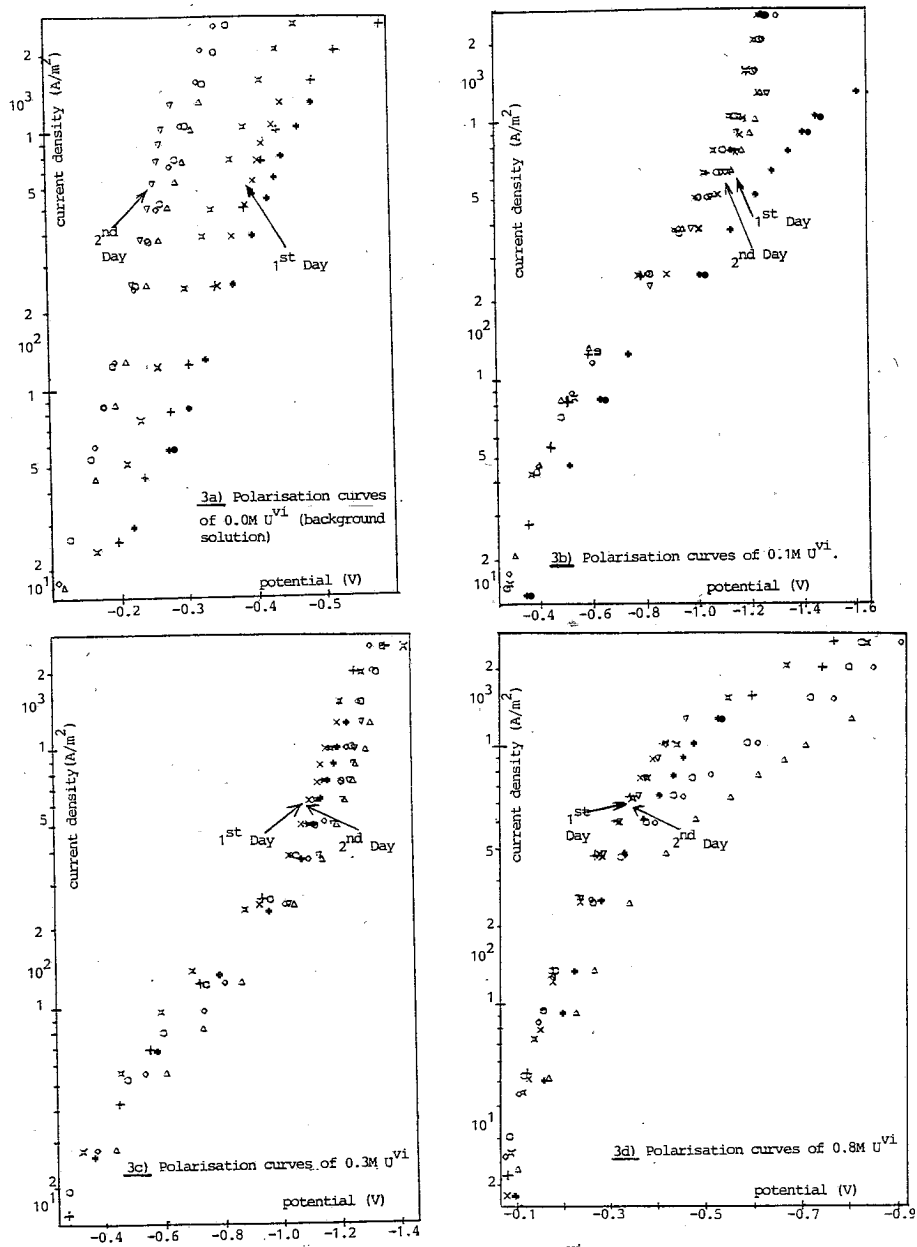

Fig (3) Polarisation curves of U^{vi} for concentrations 0.0 - 0.8M U^{vi}. The electrode was treated overnight in the solution to be examined at 600 A/m^2. The curves were taken in the following order: X immediately, after a further treatment at: ✱ 20 A/m^2 for 10 mins, ✧ 2500 A/m^2 for 15 mins, ✕ 2500 A/m^2 for 1 hr. The electrode was further treated at 600 A/m^2 overnight and the curves were repeated: ∇ immediately, at: △ 20 A/m^2 for 10 mins, ◇ 2500 A/m^2 for 15 mins, ○ 2500 A/m^2 for 1 hr. Manual sweep rate = 60 mV/min.
⟶ Cathode potential at the end of the electrode treatment.

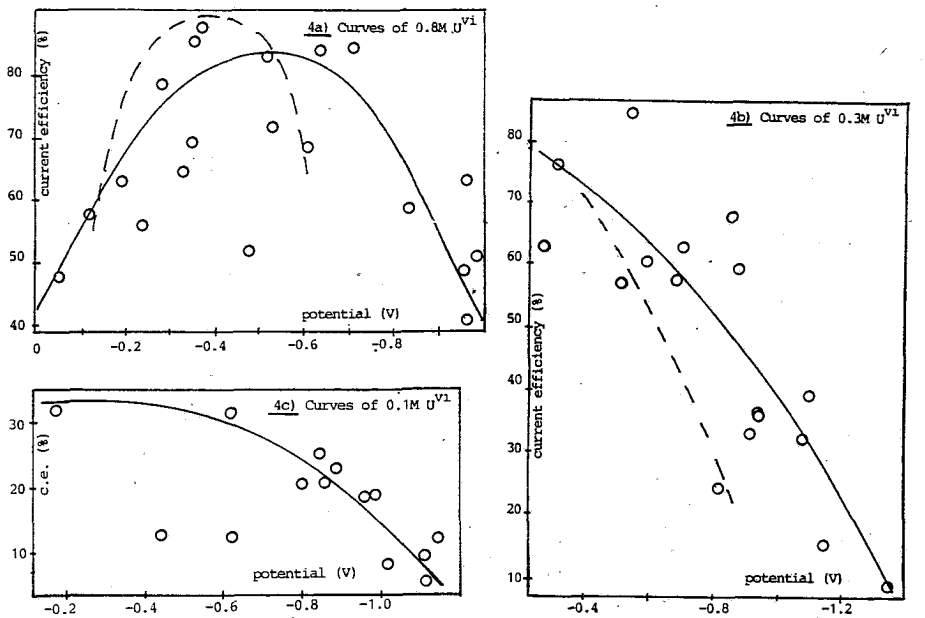

Fig (4) Current efficiency curves of U^{VI} for different concentrations (0.1 - 0.8M) on Uranium. The curves on Ti (12) are also included for comparison.

O , —— U electrode
— — —Ti electrode

Current Efficiency curves

Current efficiency curves are shown for different concentrations of U^{VI} (0.1-0.8M) in Fig 4 (a, b, c). It is seen that the curves are dependent on the concentration of U^{VI}, higher values are obtained for higher concentrations of the uranyl ion. The curve of 0.8M U^{VI} undergoes a maximum at -0.5V (S.C.E.) similar to the one obtained on Ti (12).

Comparison between U and Ti cathode materials

It has been found that U and Ti exhibit active/passive behaviour (14, 18, 20, 21) in H_2SO_4 media. The active state of the two metals has not been confirmed in HNO_3 media. The presence of two different states namely an oxide and a hydride, has been confirmed for Ti in uranyl nitrate/nitric acid solutions (12). In the present study, the presence of two different states (an oxide and the other at -1.1 V (S.C.E.) possibly active and/or hydride) has also been confirmed in similar solutions for U. Both metals have, therefore, a similar electrochemical behaviour during the electrolytic reduction of U^{VI}.

The reduction of high concentrations of uranyl nitrate takes place on an oxide surface for both metals with comparable reduction rates, Fig 5a, and current efficiencies, Fig 4a. U showed high current efficiencies for a wider potential range, Fig 4a, than Ti. The presence of an oxide film has a beneficial effect on the electrolytic reduction of U^{VI} for both metals.

The reduction of low concentrations of uranyl nitrate takes place on a hydride surface on Ti and on a non-passive surface, possibly an active and/or hydride one, on U. The reduction rates are much higher on Ti than on U, Fig 5b. U showed good current efficiencies for a wider potential range, Fig 4b, than Ti. The background polarisation curves take place on a hydride surface for Ti and on an oxide surface for U, Fig 5c.

The comparison between the two metals is made, so far, on the total reduction rates of the primary and the secondary reactions of the system. Fig 6 gives a comparison of the net reduction rate of the primary reaction only (reduction of U^{VI} to U^{IV}) between U and Ti. The comparison is based on the primary current densities excluding all contributions from the concentration of U^{VI} and the mass transfer factor according to equation (1) used for the modelling of electrochemical reactions (31).

$$i_u = \frac{1000\, c_u}{\frac{1}{2Fk_L} + \frac{1}{2Fk\, e^{-bE}}} \qquad (1)$$

where
i_u = primary current density
c_u = concentrations of U^{VI}
F = Faraday's constant
k_L = mass transfer coefficient
k,b = kinetic constants
E = cathode potential

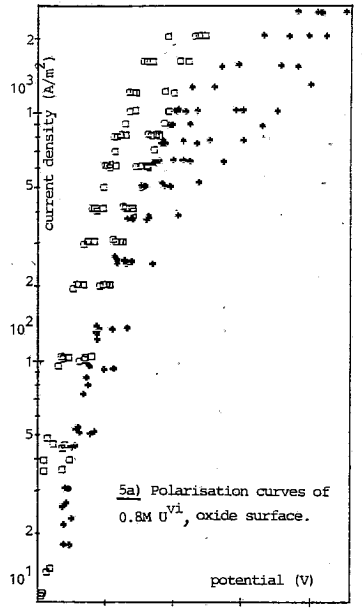

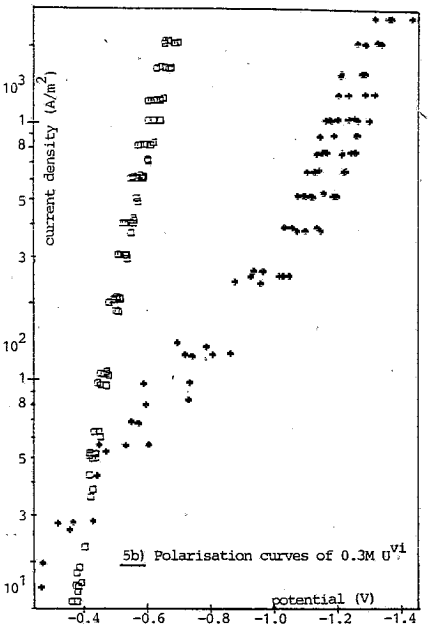

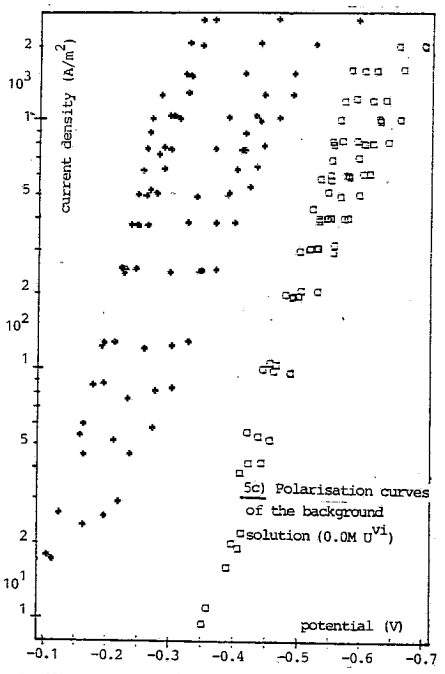

Fig (5) Comparison of the performance of U and Ti cathode materials on the electrolytic reduction of U(VI).

✱ Uranium cathode
□ Titanium cathode

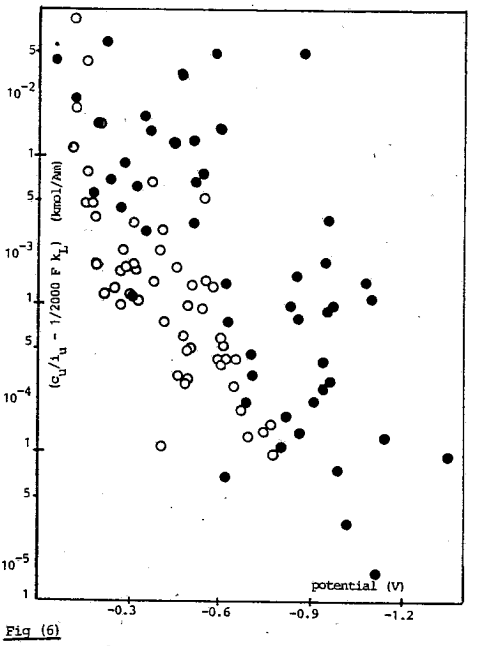

Fig (6)
Comparison of the kinetically controlled component of the primary current density on U and Ti (12). Data based on overnight preparative runs.

● U electrode ○ Ti electrode

The primary current density component, (c_u/i_u - 1/2000 Fk_L), dependent only on the kinetics of the reaction is plotted versus cathode potential on Ti and U for a wide range of concentrations of U^{VI} (0.1 - 1.0 M), shown in Fig 6. The kinetic component of the primary current density is much higher on Ti than on U, in spite of the existence of a common region. The data on Ti form a very narrow band, while the data on U are spread apart forming a very wide band. This is probably due to the existence of different states on U and the dependence of the examined reaction on the U states. All data concerning Ti in the present study are published in Ref. (12) by the same author.

Under the light of the present investigation the poor performance of the electrolytic reduction of U^{VI} on U obtained by Buckingham (29) is not very convincing.

B) *Ebonex* cathode

A preliminary examination of the Ebonex electrode surface with an electron microscope revealed the presence of an oxide film, Fig 7. Traces of an oxide film have been found even at -0.65V (S.C.E.), region of the presence of a hydride film on a Ti electrode (12).

Fig 8 shows the polarisation curves of 0.8M U^{VI} including the one of the background solution, 0.0 M U^{VI}. After an overnight treatment of the electrode at 800 A/m^2 the curve of 0.8 M U^{VI} was shifted by approx. 0.13 V towards lower cathodic potentials compared to the one taken without any previous electrochemical treatment. The shift of the polarisation curve is probably due to the formation of an oxide layer on the electrode surface. The possibility of the oxidation of the Ebonex surface during an electrolytic process has been observed by Miller (28). The observed shift (0.1V) of the polarisation curve on an Ebonex electrode has been found significantly smaller than the observed shift of approx. 0.3V on a Ti electrode (12) under similar experimental conditions.

On the following a comparison between Ebonex and Ti will be attempted based on the 0.8M data of U^{VI}. The results of Ti are taken again from a previous work of the present author (12). Ebonex showed high current efficiencies, Fig 9, which undergo a maximum in the same potential region as Ti. Ebonex showed similar current efficiency values to Ti expanded over a wider potential range than Ti, as Fig 9 demonstrates. The polarisation curve of U^{VI} on Ebonex was found similar to those on the oxide state of Ti, Fig 10. Both electrodes were electrochemically treated overnight. The reduction rates of U^{VI} to U^{IV} (excluding all secondary reactions) on Ebonex were found the same with those on the oxide state of Ti, as obtained by plotting the kinetically controlled component of the primary current density, (c_u/i_u - 1/2000 Fk_L), versus cathode potential shown in Fig 11.

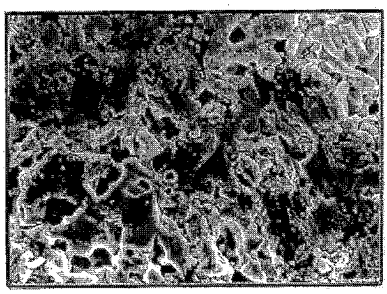

a)

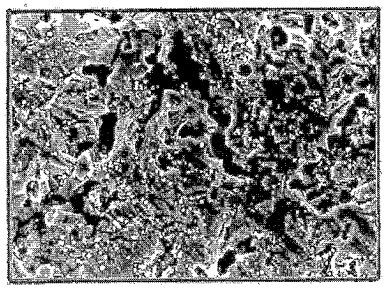

b)

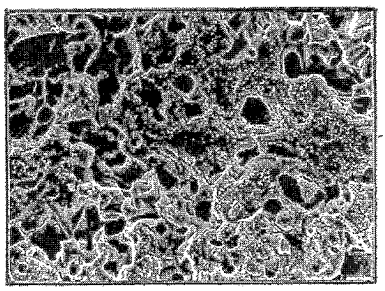

c)

Fig (7) Corrosion of the electrode surface of Ebonex during electrolysis. Photographs (x1000 magnification) taken by an electron microscope. Solution 2.0M HNO_3.

a) Before electrolysis
b) Overnight electrode treatment at -0.1V (S.C.E.)
c) Overnight electrode treatment at -0.65V (S.C.E.)

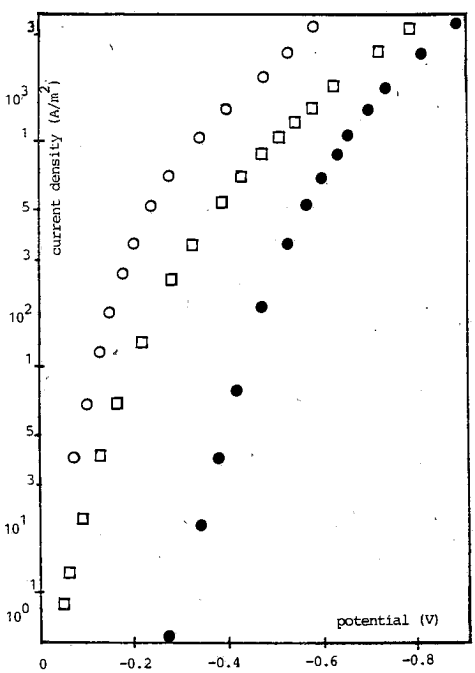

Fig (8)

Polarisation curves of 0.0M and 0.8M U^{vi} on Ebonex. Manual sweep rate = 60 mV/min.

● Curves of 0.0M U^{vi} - without electrode treatment.
□ Curves of 0.8M U^{vi} - without electrode treatment.
○ Curves of 0.8M U^{vi} - overnight electrode treatment at 800 A/m^2.

Fig (9)

Current efficiency curve of 0.8M U^{VI} on Ebonex. The curve of 0.8M U(VI) on Ti (12) is also included for comparison.

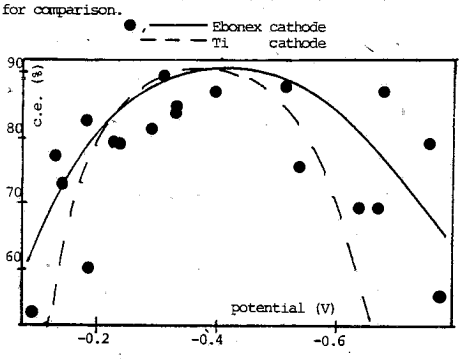

Fig (10)

Comparison of the performance of Ebonex and Ti (12) on the electrolytic reduction of U(VI).
● polarisation curve of 0.8M U(VI) on Ebonex.
○ polarisation curves of 0.8M U(VI) on Ti.

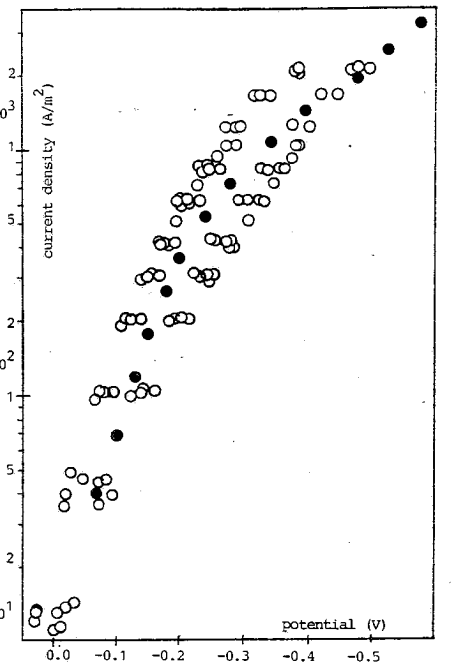

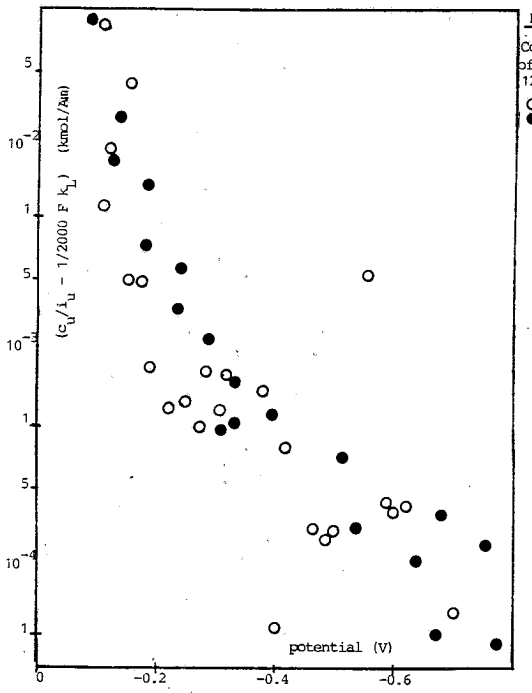

Fig (11)

Comparison of the kinetically controlled component of the primary current density on Ebonex and Ti 12). Data based on overnight preparative runs.

○ Data of U^{VI} (0.8,1.0M) on Ti
● Data of U^{VI} (0.8M) on Ebonex

CONCLUSIONS

The existence of two different states of U in uranyl nitrate/nitric acid/hydrazine solution has been confirmed in the present study. An oxide film is covering the electrode surface at low potentials. At higher potentials around -1.1 V (S.C.E.) a film of different nature is covering the electrode surface, probably a hydride film. This potential region may refer to the active state. The transition of the oxide to the other state may take place at -0.9V (S.C.E.).

The electrolytic reduction of U^{VI} on U showed high current efficiencies similar to Ti, spreading on a wider potential region. The reduction rates of U^{VI} on the oxide surface of U are similar to those of the oxide state of Ti. The other state of U (at ~ -1.1V) showed lower reduction rates (up to 100x smaller) than the equivalent of the hydride surface of Ti. This could be a serious disadvantage of U against Ti.

Ebonex is a recently invented electrode material. Although it was designed to be resistant against corrosion it was found to be oxidised during the electrolytic process to a less extent than Ti. It's electrochemical behaviour is similar to the one of the oxide state of Ti, showing the same current efficiencies and reduction rates of U^{VI}. The presence of a hydride film was not detected in the present study. The observed high reduction rates and high current efficiencies, similar to those of the oxide state of Ti, combined with the high resistivity of the material against corrosion, makes Ebonex a very promising cathode material.

SUMMARY

ΗΛΕΚΤΡΟΧΗΜΙΚΗ ΑΝΑΓΩΓΗ ΤΟΥ U^{VI} ΣΕ ΚΑΘΟΔΟΥΣ ΑΠΟ U ΚΑΙ EBONEX

Η εργασία αυτή έγινε για να μελετηθεί η ηλεκτροχημική αναγωγή του U^{VI} σε καθόδους από U και Ebonex. Τόσο το U όσο και το Ebonex δεν έχουν ξαναχρησιμοποιηθεί σαν υλικά καθόδου κατά το παρελθόν και η συμπεριφορά τους παραμένει πρακτικά άγνωστη. Το Ebonex είναι ένα κεραμικό υλικό φτιαγμένο από οξείδια του Ti (Ti_4O_7 και/ή Ti_5O_9) με μεγάλη ανθεκτικότητα στην οξείδωση και με πολύ καλή αγωγιμότητα. Η επιφάνεια του U επηρεάζεται κατά την διάρκεια της ηλεκτρόλυσης από τις πειραματικές συνθήκες και η επιφάνεια του μετάλλου ευρίσκεται συνήθως σε δύο διαφορετικές φάσεις οι οποίες πιστοποιήθησαν στην παρούσα μελέτη. Το U παρουσίασε αρκετά καλές αποδόσεις ηλεκτρικού φορτίου, ισάξιες του Ti. Η αναγωγική κινητική συμπεριφορά του U^{VI} στην οξείδια φάση του U ήταν αρκετά ικανοποιητική, ισάξια του Ti. Η δεύτερη όμως φάση του U, ο προσδιορισμός της οποίας παραμένει πρός το παρόν άγνωστος, δεν έδειξε ικανοποιητικές ταχύτητες, γεγονός που θεωρείται μειονέκτημα για το μέταλλο. Το Ebonex έδειξε πολύ ικανοποιητικές αναγωγικές ταχύτητες του U^{VI} και αποδόσεις ηλεκτρικού φορτίου ισάξιες με εκείνες του Ti. Οι ιδιότητες αυτές σε συνδυασμό μάλιστα με την ελαττωμένη οδείδωση του σε σχέση με το Ti το καθιστούν υλικό καθόδου με μεγάλες προοπτικές.

ACKNOWLEDGEMENTS

I would like to express my sincere gratitude to Prof. F. Goodridge and Dr. R.E. Plimley for their help and advice during the experimental work. I would also like to thank Mr. E. Hosley and his team for their technical support and Mr. H. Sargent for the examination of the specimens and the photographs using the electron microscope. My acknowledgements are extended to B.N.F.L. for the financial support of the present work.

REFERENCES

1. Rydberg, J., *Acta Chem. Scand* 11 (1957) 201
2. Rydberg, J., *J. Inorg. Nucl. Chem.* 5 (1957) 79.
3. Schneider, A., Wahlig, B.G., *Actinide Separations*, A.C.S. Symp. Ser. No 117 (1980) 279.
4. Baumgartner, F., Schmieder, H., *Radiochimica Acta* 25 (1978) 191.
5. Regnaut, P., *Proceedings of the 2nd United Nations, International Conference on the Peaceful Uses of Atomic Energy*, Geneva, 1958, Vol 17, p73.
6. Baumgartner, F., Ertel, D., *J. Radioanal. Chem.* 58 (1980) 11.
7. Schlea, C.S., et. al., *Du Pont de Nemours (E.I.) and Co, Savannah River Lab. AIKEN, S.C.*, Apr. 1963 DP-808.
8. Mc Kay, H.A.C., Edwall, B., De Leone, R., *Aqueous Reprocessing Chemistry of Irradiated Fuels, Brussels, Symposium 1963, European Company for the Chemical processing of the Irradiated Fuels*, p 281-293.
9. Mc Kay, H.A.C., Streeton, R.J.W., Wain, A.G., *Atomic Energy Research Establishment*, Harwell, Berkshire 1963, AERE - R4381.
10. Mastragostino, M., Saveant, J. M., *Electrochim. Acta* 13 (1968) 751.
11. Tyrovolas, Y., *Ph. D. Thesis*, University of Newcastle upon Tyne, U.K. (1989).
12. Tyrovolas, Y., *Chim.Chron. N.S.*
13. Harrison, J.A., Plimley, R.E., Tyrovolas, J., *J. Electroanal. Chem.* 225 (1987) 139.
14. Kelly, E.J., *"Modern Aspects of Electrochemistry"* No 14 Ed, J.O.' M. Bockris, B.E. Conway, R.E. White.
15. Sukhotin, A.M., Tungusova, L.I., *Prot. Met.* 4 (1968) 5.
16. Stern, M., *J. Electrochem. Soc.* 105 (1968) 638.
17. Jouve, G., Aucouturier, M., Lacombe, P., *C.R. Acad. Sc. Paris*, Ser. C. (1971) 598.
18. Kindlimann, L.E., Greene, N.D., *Corrosion - NACE* (1967) 29.
19. Shpovalov, E.T., Gerasimov, V.V., *At. Energ.* 27 (1969) 1045.
20. Ward, J.W., Waber, J.T., *J. Electrochem. Soc.* 109 (1962) 76.
21. Jenks, G.H., ORNL-4651, *Union Carbide, Corporation Nuclear Division, Oak Ridge National Laboratory, Oak Ridge*, Tenesse, June 1971.
22. Nicol, M.J., Needes, C.R.S., *Electrochim. Acta*, 20 (1975) 585.
23. Baker, M.Mc.D., Leis, L.N., Orman, S., *Trans Faraday Soc.* 62 (1966) 2513.
24. Llewelyn Leach, J.S., Nehru, A.Y., J. Electrochem. Soc. 111 (1964) 781.
25. Llewelyn Leach, J.S., *J. Inst. Met.* 88 (1959-60) 24.
26. Technical prospectus, *Ebonex technologies Inc. ICI* May (1987).
27. Hayfield, P.C.S., *US Patent* 4, 422, 917 (1983).
28. Miller, R.R., *M.Sc. Thesis, Wake Forest University*, U.S.A. (1987).
29. Buckingham, J.S., Colvin, C.A., Goodall, C.A., *HW-59283* (1959).
30. Ondrejcin, R.S., *AEC Research and Development Report, Du Pont de Nemours, (E.I.) and Co, Savannah River Lab, AIKEN, S.C.*, July 1961, DP-602.
31. Goodridge, F., *J. Chem. Tech. Biotechnol.* 38 (1987) 127-42.
32. Pollock, R.J., et. al., *Mater. Res. Bull.* 19 (1984) 17.
33. Tyrovolas, Y., to be published.

CHIMIKA CHRONIKA, *NEW SERIES*

CONTENTS

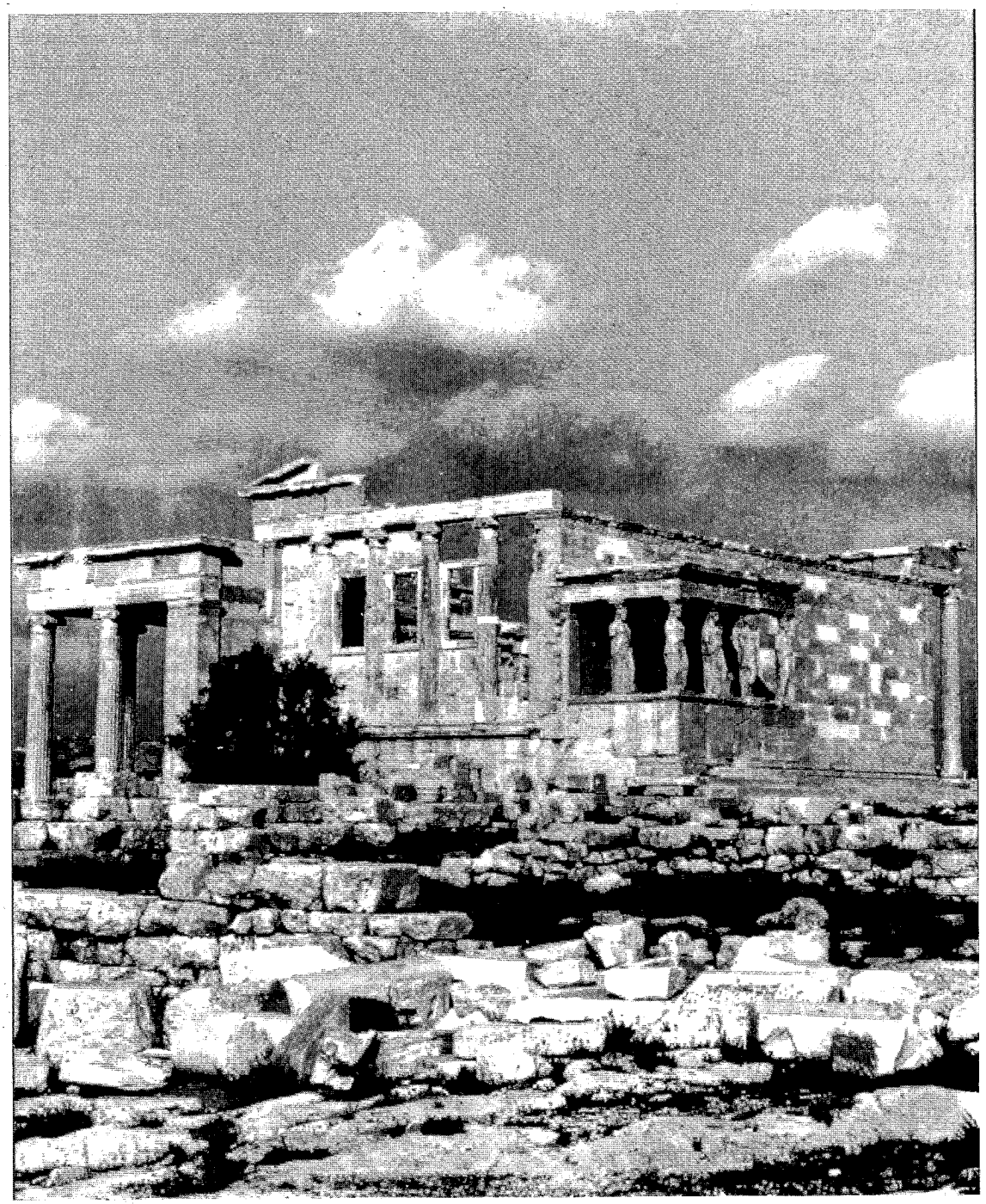

ΟΛΥΜΠΙΑΚΗ ΑΕΡΟΠΟΡΙΑ

ΑΡΧΑΙΑ ΚΟΡΙΝΘΟΣ

Hellas

ΕΛΛΗΝΙΚΟΣ ΟΡΓΑΝΙΣΜΟΣ ΤΟΥΡΙΣΜΟΥ